Congenital abnormalities of the posterior fossa

Bosemani, Thangamadhan ; Orman, Gunes ; Boltshauser, Eugen ; Tekes, Aylin ; Huisman, Thierry A G M ; Poretti, Andrea

Abstract: The frequency and importance of the evaluation of the posterior fossa have increased significantly over the past 20 years owing to advances in neuroimaging. Nowadays, conventional and advanced neuroimaging techniques allow detailed evaluation of the complex anatomic structures within the posterior fossa. A wide spectrum of congenital abnormalities has been demonstrated, including malformations (anomalies due to an alteration of the primary developmental program caused by a genetic defect) and disruptions (anomalies due to the breakdown of a structure that had a normal developmental potential). Familiarity with the spectrum of congenital posterior fossa anomalies and their well-defined diagnostic criteria is crucial for optimal therapy, an accurate prognosis, and correct genetic counseling. The authors discuss the spectrum of posterior fossa malformations and disruptions, with emphasis on neuroimaging findings (including diagnostic criteria), neurologic presentation, systemic involvement, prognosis, and risk of recurrence.

DOI: https://doi.org/10.1148/rg.351140038

Congenital Abnormalities of the Posterior Fossa[1]

Thangamadhan Bosemani, MD
Gunes Orman, MD
Eugen Boltshauser, MD
Aylin Tekes, MD
Thierry A. G. M. Huisman, MD
Andrea Poretti, MD

Abbreviations: CHARGE = *c*oloboma, *h*eart defect, choanal *a*tresia, *r*etarded growth and development, *g*enital abnormality, and *e*ar abnormality, CMV = cytomegalovirus, CSF = cerebrospinal fluid, DWM = Dandy-Walker malformation, OMIM = Online Mendelian Inheritance in Man, PCH = pontocerebellar hypoplasia

RadioGraphics 2015; 35:200–220

Published online 10.1148/rg.351140038

Content Codes: CT HN MR NR PD

[1]From the Section of Pediatric Neuroradiology, Division of Pediatric Radiology, Russell H. Morgan Department of Radiology and Radiological Science, Johns Hopkins University School of Medicine, Charlotte R. Bloomberg Children's Center, Sheikh Zayed Tower, Room 4174, 1800 Orleans St, Baltimore, MD 21287-0842 (T.B., G.O., A.T., T.A.G.M.H., A.P.); and Department of Pediatric Neurology, University Children's Hospital, Zurich, Switzerland (E.B., A.P.). Recipient of a Certificate of Merit award for an education exhibit at the 2013 RSNA Annual Meeting. Received February 17, 2014; revision requested May 16 and received June 9; accepted July 7. For this journal-based SA-CME activity, the authors, editor, and reviewers have disclosed no relevant relationships. **Address correspondence to** A.P. (e-mail: *aporett1@jhmi.edu*).

SA-CME LEARNING OBJECTIVES

After completing this journal-based SA-CME activity, participants will be able to:

- Discuss the importance of precise diagnosis of congenital posterior fossa anomalies.
- Describe the relevant neuroimaging findings using a detailed anatomic description to classify and categorize various anomalies.
- List the clinical, genetic, and prognostic factors that can help improve communication with clinicians and patients.

See www.rsna.org/education/search/RG.

The frequency and importance of the evaluation of the posterior fossa have increased significantly over the past 20 years owing to advances in neuroimaging. Nowadays, conventional and advanced neuroimaging techniques allow detailed evaluation of the complex anatomic structures within the posterior fossa. A wide spectrum of congenital abnormalities has been demonstrated, including malformations (anomalies due to an alteration of the primary developmental program caused by a genetic defect) and disruptions (anomalies due to the breakdown of a structure that had a normal developmental potential). Familiarity with the spectrum of congenital posterior fossa anomalies and their well-defined diagnostic criteria is crucial for optimal therapy, an accurate prognosis, and correct genetic counseling. The authors discuss the spectrum of posterior fossa malformations and disruptions, with emphasis on neuroimaging findings (including diagnostic criteria), neurologic presentation, systemic involvement, prognosis, and risk of recurrence.

Introduction

Over the past 2 decades, significant advances in pre- and postnatal neuroimaging techniques, the development of next-generation genetic sequencing, and an increase in animal model research have led to more accurate definition and classification of congenital abnormalities of the posterior fossa and a better understanding of their pathogenesis. Classifications of congenital posterior fossa abnormalities based on neuroimaging, molecular genetic, and developmental biologic criteria have been proposed (1–3).

Congenital posterior fossa anomalies may result from inherited (genetic) or acquired (disruptive) causes (4,5). A *malformation* is defined as a congenital morphologic anomaly of a single organ or body part due to an alteration of the primary developmental program caused by a genetic defect (6). Gene mutations causing malformations may be de novo (ie, new in the affected child, rather than present in or transmitted by the parents) or inherited from the parents. Inherited mutations are transmitted in different patterns (eg, autosomal recessive, X linked) with differences in recurrence risk for further offspring and for potential transmission of mutations from the patients to their children. The latter is the case for autosomal recessive–inherited diseases (from an unaffected mother or father to her or his child), autosomal dominant–inherited diseases (from an affected mother or father to her or his child), X-linked diseases (from an affected mother to her son), and mitochondrially inherited diseases (from an affected mother to her child). A *disruption* is defined as a congenital morphologic anomaly caused by the breakdown of an anatomic structure that had a normal developmental potential (6). Disruptive causes include prenatal infection, hemorrhage, and ischemia, among others. Disruptions are acquired lesions without risk of

TEACHING POINTS

- A *malformation* is defined as a congenital morphologic anomaly of a single organ or body part due to an alteration of the primary developmental program caused by a genetic defect. Gene mutations causing malformations may be de novo (ie, new in the affected child, rather than present in or transmitted by the parents) or inherited from the parents. Inherited mutations are transmitted in different patterns (eg, autosomal recessive, X linked) with differences in recurrence risk for further offspring and for potential transmission of mutations from the patients to their children. The latter is the case for autosomal recessive–inherited diseases (from an unaffected mother or father to her or his child), autosomal dominant–inherited diseases (from an affected mother or father to her or his child), X-linked diseases (from an affected mother to her son), and mitochondrially inherited diseases (from an affected mother to her child). A *disruption* is defined as a congenital morphologic anomaly caused by the breakdown of an anatomic structure that had a normal developmental potential. Disruptive causes include prenatal infection, hemorrhage, and ischemia, among others. Disruptions are acquired lesions without risk of recurrence. However, a genetic predisposition to disruptive lesions such as dominant mutations in *COL4A1* may be present.
- Each part of the cerebellum (vermis and hemispheres) may be hypoplastic and/or dysplastic, resulting in global cerebellar involvement or predominantly vermian involvement. Predominant involvement of the cerebellar hemispheres is uncommon and is characteristic of pontocerebellar hypoplasia as defined by Barth, as well as disruptive cerebellar development in very premature newborns. Typically, posterior fossa malformations involve both cerebellar hemispheres equally. Hypoplasia and/or dysplasia of only one cerebellar hemisphere is most likely a sequela of a prenatal disruptive lesion such as hemorrhage.
- To classify malformations that do not meet the criteria for DWM, terms such as "Dandy-Walker variant," "Dandy-Walker complex," or "Dandy-Walker spectrum" have been introduced in the past. However, these terms lack specificity and can create considerable confusion. Accordingly, these terms should not be used, and a more detailed anatomic descriptor (eg, *inferior cerebellar vermis* or *global cerebellar hypoplasia*) is to be preferred.
- The "molar tooth sign" is the diagnostic criterion for Joubert syndrome and consists of elongated, thickened, and horizontally oriented superior cerebellar peduncles; a deep interpeduncular fossa; and vermian hypoplasia.
- Cerebellar injury occurs in up to 20% of preterm infants prior to 32 weeks gestation. Impaired cerebellar development in preterm newborns may be caused by primarily destructive injuries or secondary lesions. Primarily destructive injuries include hemorrhage and ischemia and cause cerebellar tissue loss. Secondary lesions lead to underdevelopment of the cerebellum and are caused by direct (eg, hemosiderin–blood products, glucocorticoid exposure, undernutrition) or indirect (impaired transsynaptic trophic effects) effects on the cerebellum.

recurrence. However, a genetic predisposition to disruptive lesions such as dominant mutations in *COL4A1* may be present (7).

Accurate diagnoses of these complex abnormalities are of paramount significance for three primary reasons: to determine *(a)* inheritance pattern and risk of recurrence, *(b)* involvement of other systems (eg, kidneys and liver), and *(c)* prognostic implications for the child and his or her family. There are major implications for genetic counseling and family planning secondary to the significant difference in recurrence risk between a malformation and a disruption. Neuroimaging plays a key role in the diagnosis of posterior fossa abnormalities, and the challenge for the neuroradiologist is to provide the clinician with precise and up-to-date diagnostic information.

In this article, we discuss congenital posterior fossa abnormalities in terms of the normal anatomy of the posterior fossa, imaging techniques and strategy, and the most important congenital abnormalities of the posterior fossa, making use of a simple classification scheme based on the neuroimaging-based scheme proposed by Doherty et al (8). For each disorder, we summarize the key neuroimaging findings that are needed for the diagnosis and review the pattern of inheritance, systemic involvement, and long-term neurologic prognosis to emphasize the high clinical relevance of an accurate diagnosis. Although cerebellar agenesis and global cerebellar hypoplasia may result from either a malformation or a disruption, we discuss these disease entities only under "Cerebellar Disruptions" to avoid overlap.

Normal Posterior Fossa Anatomy

Conventional magnetic resonance (MR) imaging allows detailed evaluation of the anatomy of the posterior fossa and its contents (8). A midline sagittal T1- or T2-weighted sequence is ideal for showing the size of the posterior fossa, the shape and size of the vermis, and the size and morphology of the fourth ventricle and brainstem (Fig 1a). The vermis is divided into three parts by the primary and prepyramidal fissures. The rostrocaudal length of the ventral pons should be approximately twice that of the midbrain from the isthmus (ventral midbrain–pons junction) to the third ventricle, whereas the rostrocaudal length of the midbrain should be roughly the same as that of the medulla (from the level of the obex to the level of the ventral pontomedullary junction) (8). The posterior margin of the brainstem extending from the caudal aqueduct to the obex should be a straight line. The fastigium, or summit of the fourth ventricle, should lie just below the midpoint of the ventral pons on sagittal images. The cerebellar hemispheres and peduncles can be assessed on parasagittal images, whereas the size and morphology of the vermis, cerebellar hemispheres, dentate nuclei, and superior and middle cerebellar peduncles can be evaluated on axial images. In addition, the cerebellar folia run parallel to the calvaria (onion-like configuration) (Fig 1b). The individual cerebellar folia are grouped together as lobules arising from a common ray of medullary white matter. The 10 lobules of the

Figure 1. Normal anatomy of the posterior fossa in a 17-year-old girl. **(a)** Midsagittal T1-weighted MR image shows a normal-sized posterior fossa, a normal vermis, an appropriate-sized pons (rostrocaudal length approximately twice that of the midbrain and medulla), a flat dorsal surface of the brainstem (line), a normal position of the fastigium just below the midpoint of the ventral pons (black arrowhead), and primary (arrow) and prepyramidal (white arrowhead) fissures separating the vermis into three segments. **(b)** Axial T2-weighted MR image of the posterior fossa shows normal orientation of the cerebellar folia, which run parallel to the calvaria ("onion-like" orientation) (arrows). **(c)** Coronal T2-weighted MR image of the posterior fossa shows cerebellar fissures radiating toward the nuclei (arrows). **(d)** Axial color-coded fractional anisotropic map obtained at the level of the lower pons shows the middle cerebellar peduncles (anteroposterior orientation) (green) lateral to the brainstem (white arrows), anteriorly situated corticospinal tracts (superoinferior orientation) (blue) (black arrows), and posteriorly situated medial lemnisci (arrowheads), with the transverse pontine fibers (transverse orientation) in between (red) (*). **(e)** Axial color-coded fractional anisotropic map obtained at the level of the pontomesencephalic junction shows the superior cerebellar peduncles (green-blue) (arrows) and transverse fibers at the decussation of the ventral tegmentum and superior cerebellar peduncles (red) (arrowhead).

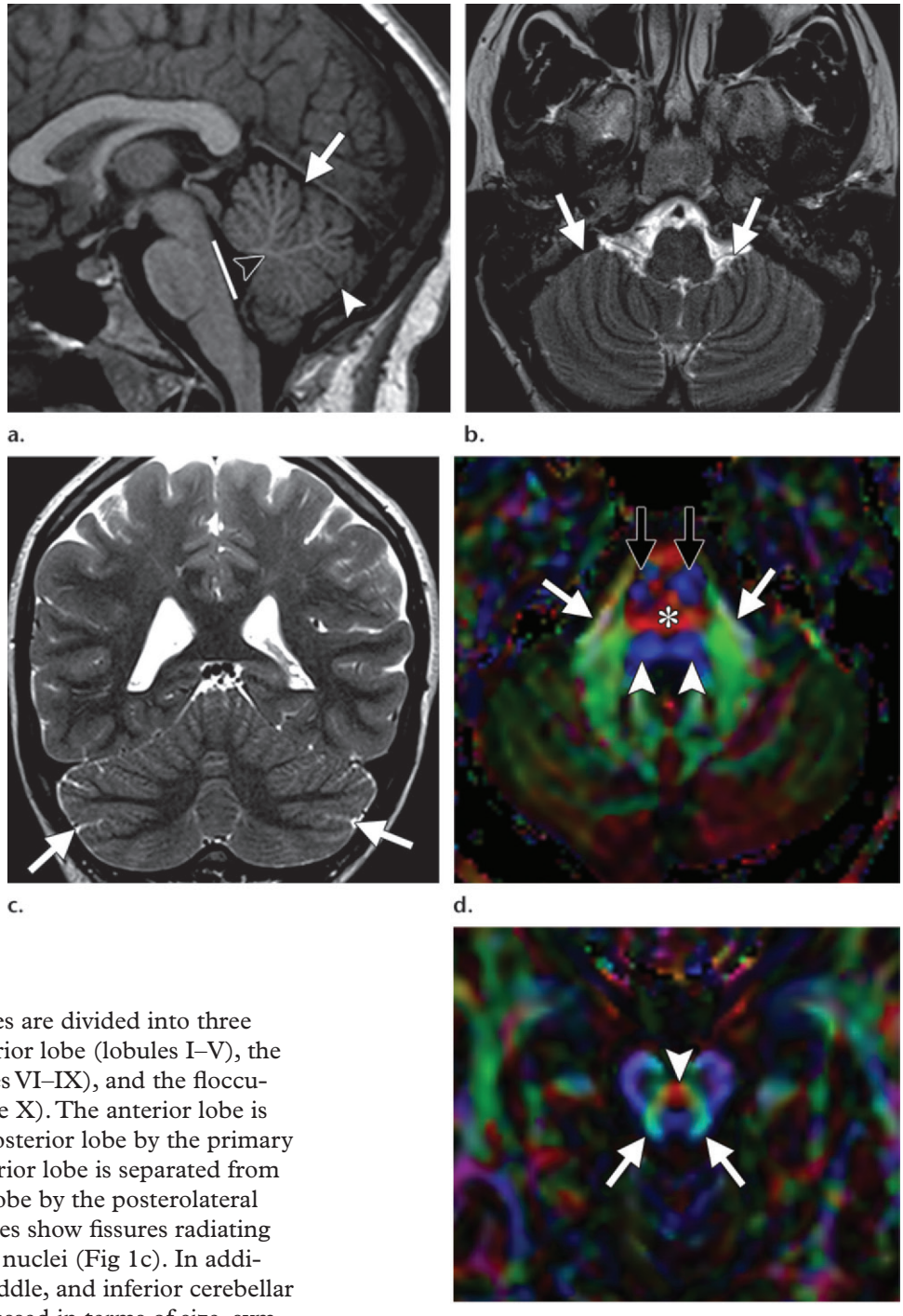

cerebellar hemispheres are divided into three major lobes: the anterior lobe (lobules I–V), the posterior lobe (lobules VI–IX), and the flocculonodular lobe (lobule X). The anterior lobe is separated from the posterior lobe by the primary fissure, and the posterior lobe is separated from the flocculonodular lobe by the posterolateral fissure. Coronal images show fissures radiating toward the cerebellar nuclei (Fig 1c). In addition, the superior, middle, and inferior cerebellar peduncles can be assessed in terms of size, symmetry, contour, and location.

Table 1: Role of MR Imaging Sequences in the Evaluation of the Pediatric Posterior Fossa

Sequence	Plane	Key Applications
3D T1W	Axial, coronal, sagittal	Excellent differentiation between gray matter and white matter, acquisition of high-resolution anatomic information
T2W	Axial, coronal	Acquisition of high-resolution anatomic information; delineation of cortex, white matter, and gray matter nuclei
Diffusion tensor	Axial	Evaluation of white matter microstructural integrity, identification of white matter tracts
CISS*	Axial + MPR	Evaluation of cerebellar folia, cranial nerves, ventricles, and foramina
Susceptibility-weighted	Axial	Identification and characterization of hemorrhage, blood products, calcification, and iron accumulation

Note.—CISS = constructive interference in the steady state, MPR = multiplanar reformation, 3D = three-dimensional, T1W = T1-weighted, T2W = T2-weighted.
*Optional (depending on indication).

Imaging Techniques and Strategy

Ultrasonography (US), computed tomography, and MR imaging (the only modality discussed in this article) are the key neuroimaging modalities for the evaluation of the neonatal and pediatric posterior fossa. Isotropic three-dimensional T1-weighted images allow good anatomic evaluation in three imaging planes in a reasonable amount of time. High-resolution T2-weighted images are ideal for more detailed evaluation of cerebellar folia, interfolial spaces, cerebellar cortex, gray matter–white matter differentiation, dentate nuclei, and brainstem cranial nerve nuclei. Depending on the clinical presentation, suspected diagnosis, or pathologic condition, the use of various additional sequences may be considered. Diffusion tensor imaging provides detailed qualitative and quantitative information about the microstructure and organization of the white matter tracts within the posterior fossa (Fig 1d, 1e) (9). Susceptibility-weighted imaging is highly sensitive for blood, blood products, and calcifications and may be helpful in supporting the notion of a disruptive pathomechanism (10). The indications for the essential anatomic and functional MR imaging sequences to be included in a detailed neuroimaging study of congenital posterior fossa anomalies are summarized in Table 1.

Congenital abnormalities of the posterior fossa may be diagnosed with prenatal imaging. Although fetal neuroimaging has improved markedly, prenatal diagnosis, outcome prognostication, and counseling for women carrying fetuses with congenital posterior fossa abnormalities remain fraught with difficulties. The current understanding of formation of the cerebellum seems to support the theory that development of the cerebellar vermis should be complete at around 18 weeks gestation. Accordingly, prenatal imaging before 18–20 weeks gestation may be problematic and lead to a high number of false-positive cerebellar abnormalities.

Malformations

As mentioned earlier, we classify posterior fossa malformations using a simple classification scheme based on the neuroimaging pattern proposed by Doherty et al (8). We divide these malformations into *(a)* predominantly cerebellar, *(b)* cerebellar and brainstem, *(c)* predominantly brainstem, and *(d)* predominantly midbrain malformations (Table 2). Although such a classification scheme may not be as comprehensive as a genetics- or embryology-based classification scheme, we are convinced that it is practical and accessible for daily clinical practice.

Predominantly Cerebellar Malformations

A malformed cerebellum may be hypoplastic (reduced cerebellar volume), dysplastic (abnormal cerebellar foliation, fissuration, and architecture of the cerebellar white matter), or hypodysplastic (combination of hypoplasia and dysplasia). Each part of the cerebellum (vermis and hemispheres) may be hypoplastic and/or dysplastic, resulting in global cerebellar involvement or predominantly vermian involvement. Predominant involvement of the cerebellar hemispheres is uncommon and is characteristic of pontocerebellar hypoplasia (PCH) as defined by Barth (11), as well as disruptive cerebellar development in very premature newborns. Typically, posterior fossa malformations involve both cerebellar hemispheres equally. Hypoplasia and/or dysplasia of only one cerebellar hemisphere is most likely a sequela of a prenatal disruptive lesion such as hemorrhage. In this section, besides DWM, we discuss other cystic posterior fossa malformations (Blake pouch cyst,

Table 2: Neuroimaging-based Differential Diagnosis for Congenital Posterior Fossa Abnormalities

Neuroimaging Pattern	Malformations
Predominantly cerebellar involvement	
Predominantly vermian	DWM and other cystic lesions of the posterior fossa, including Blake pouch cyst, mega cisterna magna, and arachnoid cysts; isolated vermian hypoplasia; rhombencephalosynapsis
Global cerebellar	Malformations of cortical development: lissencephaly (*RELN*, *VLDRL*, tubulin genes), polymicrogyria (tubulin genes, *GPR56*), periventricular nodular heterotopia (*FLNA*), and primary microcephaly; macrocerebellum; cerebellar dysplasia, including Chudley-McCullough syndrome; global cerebellar hypoplasia in multiple genetic syndromes (eg, Ritschcer-Schinzel syndrome, CHARGE syndrome, Delleman syndrome); congenital CMV infection
Unilateral cerebellar	Isolated unilateral cerebellar hypoplasia, PHACES syndrome, *COL4A1* mutations, cerebellar cleft
Cerebellar and brainstem involvement	PCH type 1–10; glycosylation type 1a congenital disorder; *CASK* mutations; Joubert syndrome; cerebellar agenesis caused by a disruptive lesion or representing a malformation due to *PTF1A* mutations; congenital muscular dystrophies due to defective dystroglycan *O*-glycosylation; vanishing cerebellum in Chiari 2 malformation; cerebellar disruption secondary to prematurity
Predominantly brainstem involvement	Pontine tegmental cap dysplasia; horizontal gaze palsy and progressive scoliosis (*ROBO3* mutations)
Predominantly midbrain involvement	Dysplasia of the diencephalic-mesencephalic junction

Note.—CHARGE = *c*oloboma, *h*eart defect, choanal *a*tresia, *r*etarded growth and development, *g*enital abnormality, and *e*ar abnormality, CMV = cytomegalovirus, DWM = Dandy-Walker malformation, PCH = pontocerebellar hypoplasia.

mega cisterna magna, and arachnoid cysts), although these other malformations are characterized by a normal cerebellum. Our intention is to help the reader differentiate between these malformations and a true DWM.

Dandy-Walker Malformation.—DWM is the most common posterior fossa malformation and typically occurs only sporadically, with a low overall risk of recurrence (1%–5%) (8). DWM may be isolated or may occur as part of chromosomal anomalies or well-defined Mendelian disorders such as Ritscher-Schinzel or cranio-cerebello-cardiac syndrome (Online Mendelian Inheritance in Man [OMIM] 220210). In addition, rare mutations in six genes (*ZIC1*, *ZIC4*, *FOXC1*, *FGF17*, *LAMC1*, and *NID1*) have been found in a few patients with DWM. On the basis of the function of these genes, DWM may represent a complex disruption of the interaction between the developing cerebellum and the developing posterior fossa mesenchyme and its derivates.

The majority of patients with DWM present before 1 year of age with signs and symptoms of increased intracranial pressure (12). Macrocephaly is the most common manifestation, affecting 90%–100% of children during the first months of life (13). Nowadays, the diagnosis of DWM is made prenatally in an increasing number of patients. The outcome of children with DWM is variable. Limited evidence shows that normal lobulation of the cerebellar vermis and the absence of associated brain abnormalities (particularly callosal dysgenesis) may be prognostic for normal cognitive function (14,15). Systemic involvement (eg, cardiovascular, urogenital, or skeletal anomalies) may be seen in DWM, is associated with defined syndromes, and also influences the prognosis (poorer outcome).

The key neuroimaging features of DWM are *(a)* hypoplasia (or, rarely, agenesis) of the cerebellar vermis (whose inferior portion is typically affected, possibly in combination with its superior portion), which is elevated and upwardly rotated; and *(b)* dilatation of the cystic-appearing fourth ventricle, which consequently may fill the entire posterior fossa (Fig 2a). Both findings are consistently present and are required for the diagnosis. The cystic structure within the posterior fossa is not the posterior fossa subarachnoid space or an arachnoid cyst; instead, it represents the cystlike dilatation of the fourth ventricle secondary to hypoplasia of the inferior cerebellar vermis. The cerebellar hemispheres are typically displaced anterolaterally, but their size and morphology are usually normal (9). The posterior fossa is usually enlarged, and the tentorium as well as the torcular and transverse sinuses are elevated (2).

Figure 2. Cystic malformations of the posterior fossa as seen at sagittal T1-weighted MR imaging. **(a)** Image shows a DWM with a hypoplastic vermis in upward rotation (arrow), cystic dilatation of the fourth ventricle (*) with posterior extension and communication with an enlarged posterior fossa, and supratentorial hydrocephalus (arrowhead). **(b)** Image shows a Blake pouch cyst with enlargement of the fourth ventricle, which communicates with an infravermian cystic compartment (arrow) corresponding to enlargement of the Blake pouch; a normal vermis; and supratentorial hydrocephalus (arrowhead). (Reprinted, with permission, from reference 19.) **(c)** Image shows mega cisterna magna (arrow), a normal vermis, a normal fourth ventricle, an enlarged posterior fossa, scalloping of the occipital bone, and the absence of hydrocephalus. **(d)** Image shows a retrocerebellar arachnoid cyst that is isointense relative to CSF (white arrows), with apparent enlargement of the posterior fossa, scalloping of the occipital bone, mass effect on the dorsal aspect of a normal-appearing vermis (black arrow), a normal fourth ventricle, and supratentorial hydrocephalus (arrowhead). **(e)** Image shows isolated inferior vermian hypoplasia with partial absence of the inferior vermis (arrow) and apparent but not true enlargement of the fourth ventricle.

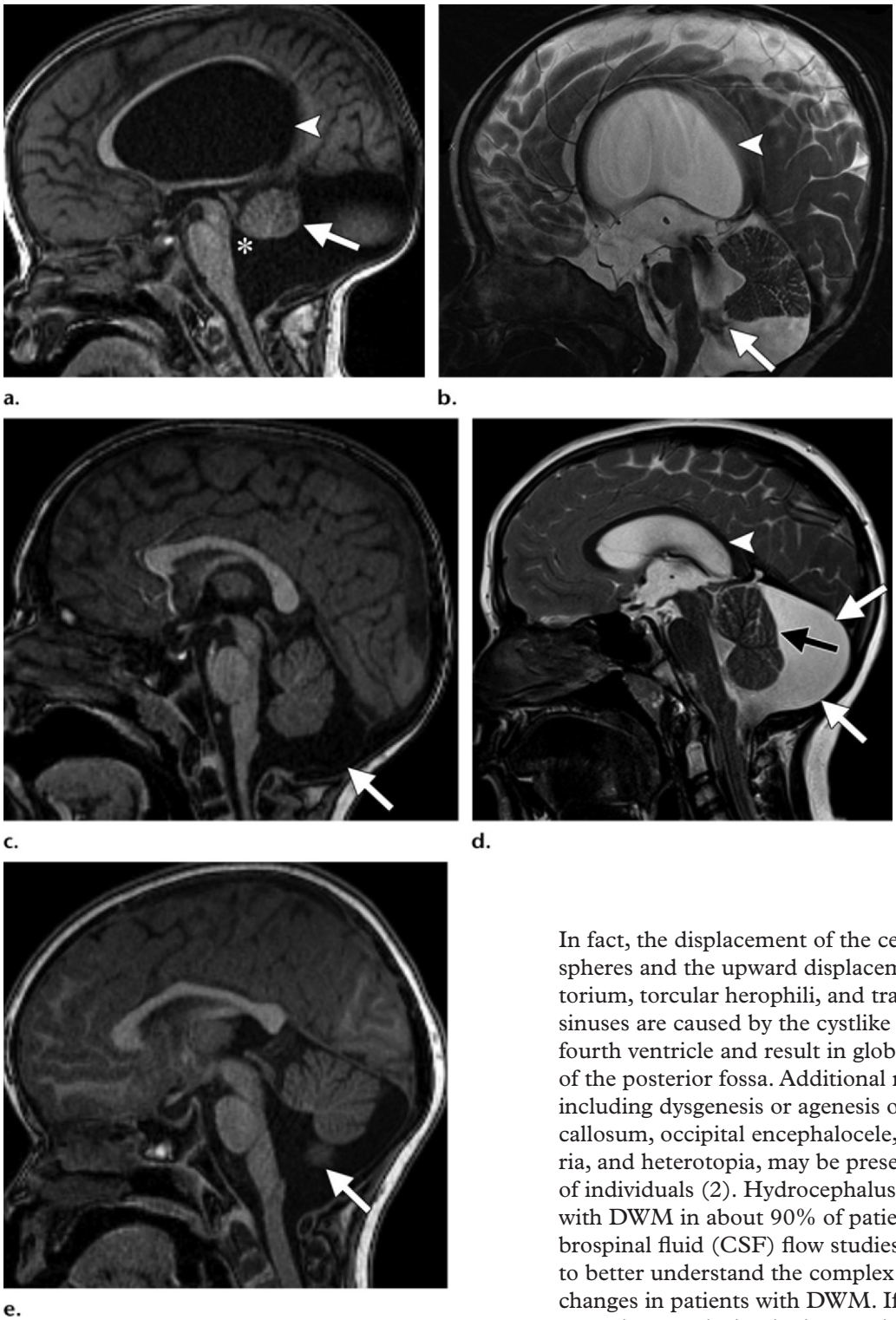

In fact, the displacement of the cerebellar hemispheres and the upward displacement of the tentorium, torcular herophili, and transverse dural sinuses are caused by the cystlike dilatation of the fourth ventricle and result in global enlargement of the posterior fossa. Additional malformations, including dysgenesis or agenesis of the corpus callosum, occipital encephalocele, polymicrogyria, and heterotopia, may be present in 30%–50% of individuals (2). Hydrocephalus is associated with DWM in about 90% of patients (2). Cerebrospinal fluid (CSF) flow studies may be added to better understand the complex hydrodynamic changes in patients with DWM. If aqueductal stenosis or occlusion is shown with CSF flow

Table 3: Key Neuroimaging Features of DWM versus Other Cystic Posterior Fossa Malformations

Malformation	Vermis	Fourth Ventricle	Posterior Fossa	Hydrocephalus	Occipital Bone Scalloping*
DWM	Hypoplastic	Enlarged	Enlarged	Yes (in most patients)	No
IVH	Hypoplastic (inferior portion)	Enlarged	Normal	No	No
BPC	Normal	Enlarged	Normal	Yes	No
MCM	Normal	Normal	Inconsistently enlarged	No	Possible
PFAC	Normal	Normal or reduced	Normal	Possible	Yes

Note.—BPC = Blake pouch cyst, IVH = isolated vermian hypoplasia, MCM = mega cisterna magna, PFAC = posterior fossa arachnoid cyst.
*Not typically seen in neonates and infants.

studies, cystoperitoneal shunt placement is not sufficient and placement of a ventriculoperitoneal shunt is required.

Neuroimaging diagnostic criteria usually make it possible to distinguish DWM from other cystic posterior fossa malformations (Table 3). In some patients, however, only a partial neuroimaging phenotype of DWM is noted. To classify malformations that do not meet the criteria for DWM, terms such as "Dandy-Walker variant," "Dandy-Walker complex," or "Dandy-Walker spectrum" have been introduced in the past. However, these terms lack specificity and can create considerable confusion. Accordingly, these terms should not be used, and a more detailed anatomic descriptor (eg, *inferior cerebellar vermis* or *global cerebellar hypoplasia*) is to be preferred (2).

***Blake Pouch Cyst.*—**Blake pouch cyst is caused by lack of fenestration of the Blake pouch, resulting in absence of communication between the fourth ventricle and the subarachnoid space (16–18) and leading to tetraventricular hydrocephalus. The cerebellum has a normal size and shape. Blake pouch cyst occurs sporadically, and no recurrence risk has been reported.

Hydrocephalus and macrocephaly are the most common presenting features in the neonatal period (18). The long-term outcome depends mostly on complications related to neurosurgical procedures. In the absence of shunt-related complications, the prognosis is generally favorable.

Typical neuroimaging findings include the presence of a cyst in a retrocerebellar or infraretrocerebellar location, which is essentially a diverticulum of the consequently enlarged fourth ventricle (Fig 2b). The presence of this cyst is responsible for the displacement of the choroid plexus inferior to the vermis along the anterosuperior aspect of the cyst. The displacement of the choroid plexus is best visualized as an enhancing structure on sagittal contrast material–enhanced T1-weighted images (17). The consistent presence of hydrocephalus allows the differentiation of Blake pouch cyst from mega cisterna magna. Mild mass effect may result in indentation of the inferior vermis or of the caudal and medial aspects of the cerebellar hemispheres. The posterior fossa is typically normal in size. Supratentorial morphologic abnormalities other than hydrocephalus are usually absent.

***Mega Cisterna Magna.*—**Mega cisterna magna is an enlarged cisterna magna (≥10 mm on midsagittal images) with an intact vermis, a normal fourth ventricle, and, in some patients, an enlarged posterior fossa (Fig 2c) (16,20,21). It represents a truly focal enlargement of the subarachnoid space in the inferior and posterior portions of the posterior fossa. Consequently, mega cisterna magna freely communicates with the fourth ventricle and the cervical subarachnoid space, which is confirmed with CSF flow studies (20) and results in consistent absence of hydrocephalus. It has been suggested that delayed fenestration of the Blake pouch results in mega cisterna magna, whereas the absence of fenestration of the Blake pouch results in Blake pouch cyst (17). There is no reported recurrence risk.

Mega cisterna magna is typically an incidental finding and represents a normal variant. Accordingly, no follow-up neuroimaging studies are required. The vast majority (90%–95%) of children with isolated mega cisterna magna develop normally (15).

Neuroimaging plays a key role in identifying mega cisterna magna and in differentiating it from isolated inferior vermian hypoplasia and Blake pouch cyst. In mega cisterna magna, the presence of a normal vermis and the absence of

hydrocephalus help differentiate it from isolated inferior vermian hypoplasia and Blake pouch cyst, respectively.

Posterior Fossa Arachnoid Cysts.—Duplications of the arachnoid membrane produce fluid-filled cysts known as arachnoid cysts. About 10% of arachnoid cysts in children occur in the posterior fossa and may be located inferior or posterior to the vermis in a midsagittal location (retrocerebellar), cranial to the vermis in the tentorial hiatus (supravermian), anterior or lateral to the cerebellar hemispheres, or anterior to the brainstem (22). Arachnoid cysts do not communicate with the fourth ventricle or the subarachnoid space. There is no reported recurrence risk.

Macrocephaly, signs of increased intracranial pressure, and developmental delay are possible clinical findings in children with posterior fossa arachnoid cysts, particularly if CSF flow is obstructed (23). However, these cysts may be asymptomatic and discovered incidentally. Overall, children who undergo surgery and shunt placement have a favorable outcome (4,23).

Neuroimaging reveals a well-circumscribed extraaxial fluid collection or cyst that is isointense relative to CSF with all sequences (Fig 2d). The presence of proteinaceous content may lead to lack of complete signal suppression with a fluid-attenuated inversion-recovery sequence. Diffusion-weighted imaging reveals free water motion or facilitated diffusion similar to that seen in CSF. The cyst walls are usually too thin to be visualized at MR imaging. Arachnoid cysts may enlarge during infancy and produce mass effect on the cerebellum and vermis, which may cause a secondary obstruction of the ventricular system, hydrocephalus, and/or remodeling or thinning of the overlying occipital bone.

Isolated Inferior Vermian Hypoplasia.—Isolated inferior vermian hypoplasia is a pathologic condition that is characterized by partial absence of the inferior portion of the cerebellar vermis. In the literature, there is some confusion about isolated inferior vermian hypoplasia, with some authors referring to it as Dandy-Walker variant (24). As discussed earlier, the term *Dandy-Walker variant* lacks specificity, creates confusion, and can lead to misdiagnosis and incorrect genetic counseling. Inferior vermian hypoplasia in isolation has no recurrence risk; however, this condition may occur in the context of Mendelian syndromes, in which case it does carry a recurrence risk.

More than 75% of patients with isolated inferior vermian hypoplasia have a favorable outcome (25,26). In some patients, mild functional deficits in fine motor activity and receptive language may be present.

The key neuroimaging finding in isolated inferior vermian hypoplasia is partial absence of the inferior vermis, a finding that is best seen on the midsagittal image (Fig 2e). The remainder of the vermis, as well as the cerebellar hemispheres, the fourth ventricle, and the posterior fossa, have a normal size and architecture. The prenatal diagnosis of isolated inferior vermian hypoplasia is reliable after 18–20 weeks gestation (25). Before 18 weeks gestation, incomplete caudal growth of the inferior vermis over the fourth ventricle may be physiologic. The prenatal US diagnosis of inferior vermian hypoplasia is not reliable. Fetal MR imaging provides a more sensitive and specific diagnosis of inferior vermian hypoplasia compared with US, but the false-positive rate remains high (~30%) (25).

Cerebellar Involvement in Migrational Disorders.—Posterior fossa abnormalities including hypoplasia of the pons and cerebellum have been reported in migrational disorders (27). A severely hypoplastic cerebellum with a markedly reduced foliation pattern and severe hypoplasia of the pons are characteristic findings in patients with mutations in *RELN* (28) and *VLDLR* (29). Typically, the cerebellar vermis is more affected than the hemispheres. Patients with autosomal recessive mutations in *RELN* typically present with microcephaly, seizures, marked cognitive impairment, and congenital lymphedema. The supratentorial brain shows a simplified gyration pattern in the majority of patients. Patients with autosomal recessive mutations in *VLDLR* have a similar but milder posterior fossa neuroimaging phenotype compared with patients with mutations in *RELN*.

Mutations in a number of neuron-specific α- and β-tubulin genes (eg, *TUBA1A*, *TUBB2B*) are associated with a spectrum of posterior fossa abnormalities ranging from severe PCH to mild cerebellar hypoplasia, pontine cleft, and/or asymmetric cerebral peduncles (Fig 3a) (30). In addition, asymmetry of the cerebellar hemispheres and peduncles may be present. Dysmorphic basal ganglia with an abnormal internal capsule are a consistent and characteristic supratentorial finding (Fig 3b). Migrational abnormalities ranging from lissencephaly to polymicrogyria and callosal hypoplasia may also be present. The majority of mutations in tubulin genes are de novo.

Rhombencephalosynapsis.—Rhombencephalosynapsis is characterized by absence of the vermis and continuity of the cerebellar hemispheres, dentate nuclei, and superior cerebellar peduncles (31). The majority of patients are nonsyndromic. However, rhombencephalosynapsis is a key feature of Gómez-López-Hernández syndrome

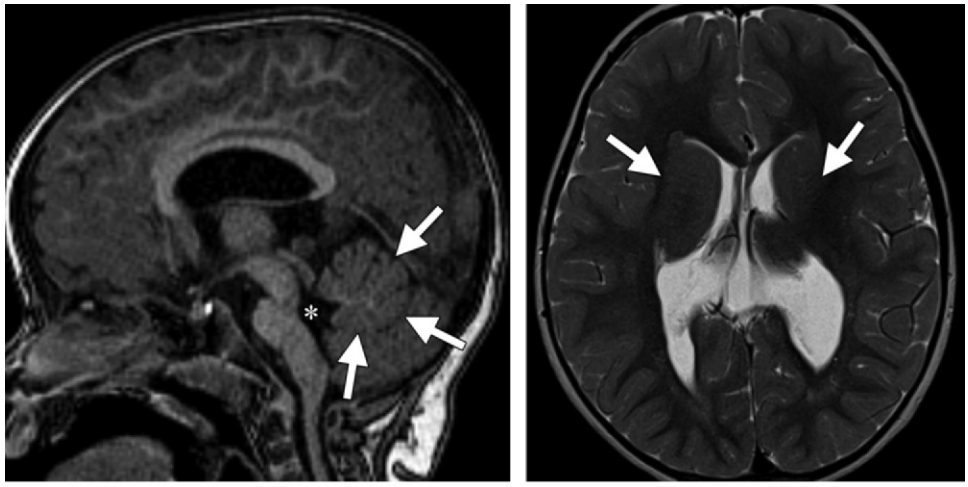

Figure 3. *TUBA1A* mutation in a 22-month-old girl who presented with developmental delay. **(a)** Sagittal T1-weighted MR image shows vermian hypoplasia (arrows), pontine hypoplasia with abnormally increased rostrocaudal length of the medulla and midbrain with respect to the pons, and loss of the normal flat dorsal surface of the brainstem (*). **(b)** Axial T2-weighted MR image shows dysmorphic caudate heads and putamina with loss of a clear interface between these structures and the internal capsule (arrows), bilateral ventriculomegaly with abnormal configuration of the anterior horns of the lateral ventricles, and no apparent cortical migrational abnormality.

(OMIM 601853 [parietal alopecia, trigeminal anesthesia, and craniofacial dysmorphic signs]) (32,33) and may be seen in patients with associated VACTERL (*v*ertebral anomalies, *a*nal atresia, *c*ardiovascular anomalies, *t*racheo*e*sophageal fistula, *r*enal anomalies, and *l*imb defects) (34). The sporadic nature of rhombencephalosynapsis contributes to its low recurrence risk.

The most common clinical manifestations of rhombencephalosynapsis include truncal and/or limb ataxia, abnormal eye movements, head stereotypies, and delayed motor development. Long-term cognitive outcome varies from severe impairment to normalcy (32). Patients with more severe rhombencephalosynapsis, associated holoprosencephaly, or VACTERL features have more severe neurodevelopmental impairment (34). Systemic involvement is uncommon.

The key neuroimaging findings in rhombencephalosynapsis are agenesis or hypogenesis of the vermis and continuity (often called fusion) of the cerebellar hemispheres, superior cerebellar peduncles, and dentate nuclei, which creates a horseshoe-shaped arch across the midline, resulting in a keyhole-shaped fourth ventricle (Fig 4). Posterior coronal T2-weighted images are crucial in showing the horizontal folial pattern (Fig 4a), whereas the midsagittal T1-weighted image depicts the dentate nuclei. (In normal anatomy, the vermis separates the dentate nuclei in the midline.) Rhombencephalosynapsis may be associated with other central nervous system anomalies such as hydrocephalus, mostly due to aqueductal stenosis and forebrain abnormalities including absent olfactory bulbs, dysgenesis of the corpus callosum, and absent septum pellucidum (34).

Macrocerebellum.—Macrocerebellum, or cerebellar hyperplasia, is an extremely rare condition that is characterized by an abnormally large cerebellum with preservation of its overall shape (35). Macrocerebellum may be isolated (nonsyndromic) or part of well-defined syndromes (eg, Costello syndrome, Sotos syndrome) or neurometabolic diseases (eg, fucosidosis, mucopolysaccharidosis type I and II) (35,36). The significant difference in pathogenesis between these disorders suggests that macrocerebellum may not be a nosologic entity, but instead represents the structural manifestation of a deeper, more basic biologic disturbance common to heterogeneous diseases. The recurrence risk of macrocerebellum depends on the underlying disorder. In patients with isolated macrocerebellum, the recurrence risk is low (35).

The clinical presentation of patients with macrocerebellum is highly heterogeneous and depends mostly on the underlying disease. Ataxia, hypotonia, intellectual disability, and ocular movement disorders are common in patients with isolated macrocerebellum.

The key neuroimaging finding of macrocerebellum is disproportionate cerebellar enlargement with preserved architecture and shape, which is best seen on sagittal or axial images (Fig 5) (35,37). The cerebellar hemispheres are more affected than the vermis and may expand into adjacent anatomic regions by wrapping around the

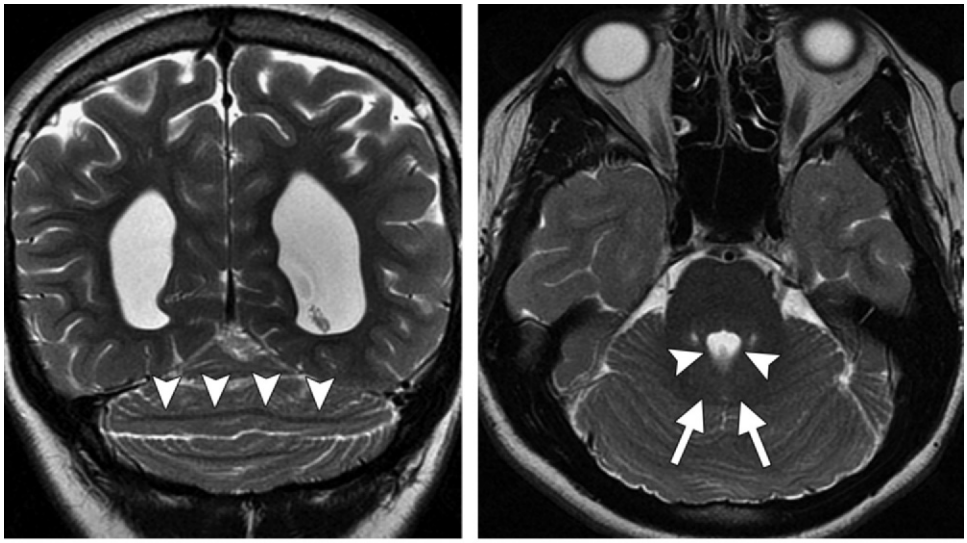

a. b.

Figure 4. Rhomboencephalosynapsis in a 5-year-old boy who presented with ataxia. **(a)** Posterior coronal T2-weighted MR image shows continuity of the cerebellar hemispheres with an abnormal transverse orientation of the cerebellar foliae (arrowheads). **(b)** Axial T2-weighted MR image shows continuity of the cerebellar hemispheres, dentate nuclei (arrows), and superior cerebellar peduncles (arrowheads) without an intervening vermis.

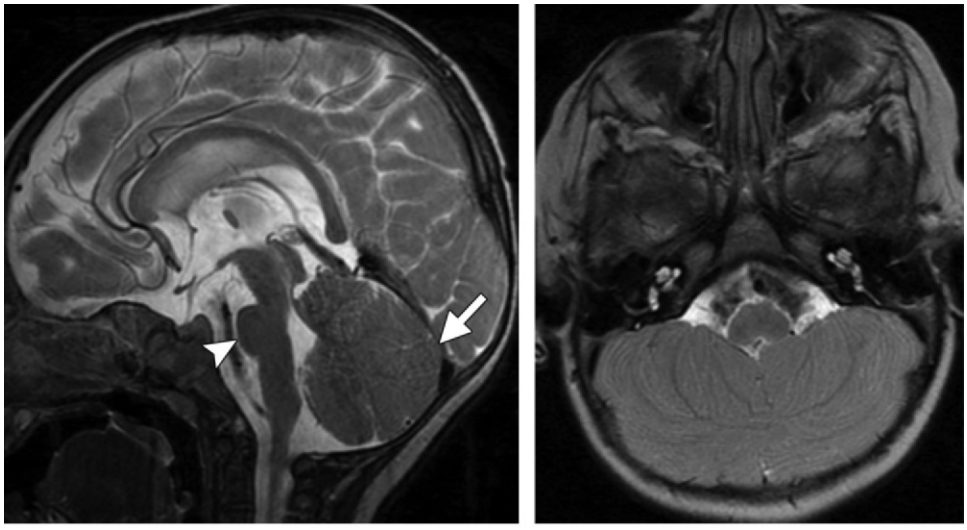

a. b.

Figure 5. Macrocerebellum in a 7-month-old patient who presented with nystagmus and delayed visual fixation. Sagittal **(a)** and axial **(b)** T2-weighted MR images show a marked increase in the size of the cerebellum (arrow in **a**), with marked thickening of the cerebellar gray matter and a normal-sized posterior fossa. The midbrain appears to be elongated and thickened, whereas the pons appears to be shortened (arrowhead in **a**). (Reprinted, with permission, from reference 37.)

brainstem or herniating upward or downward. Supratentorial findings such as ventriculomegaly or white matter signal abnormalities may be present depending on the underlying disease.

Cerebellar Dysplasia.—*Cerebellar dysplasia* is a descriptive anatomic term. This pathologic condition includes a heterogeneous distribution of different causes, both malformations and disruptions, and hence the variable clinical presentations, additional neuroimaging findings, and recurrence risks.

The clinical manifestation of cerebellar dysplasia is highly variable, ranging from an incidental finding to severe neurologic impairment.

The key neuroimaging findings of cerebellar dysplasia are abnormal foliation, fissuration (including defective, enlarged, or vertical fissures), white matter arborization, and an obscured gray matter–white matter junction (Fig 6) (38). Findings

Table 4: Subtypes of PCH

Subtype	Main Features	Genotype
1	Involvement of the anterior horn cells	*VRK1*, *TSEN54*, *RARS2*, *EXOSC3*
2	Chorea/dystonia; rarely, spasticity only	*TSEN54* (vast majority of cases); *TSEN2*, *TSEN34*
3	Optic atrophy, nonprogressive course	Locus on 7q11–21
4	Severe neonatal course with hypertonia and hypoventilation, absent inferior olivary prominence at autopsy	*TSEN54*
5	Lethal course with neonatal death, more pronounced involvement of the vermis than of the hemispheres	*TSEN54*
6	Lactic acidemia, high lactate level in CSF	*RARS2*
7	Micropenis with no palpable gonads	Unknown
8	Proportionate involvement of the vermis and hemispheres, nonprogressive course	*CHMP1A*
9	Dysgenesis of the corpus callosum	*AMPD2*
10	Dysmorphic features and axonal sensorimotor neuropathy (inconsistent)	*CLP1*

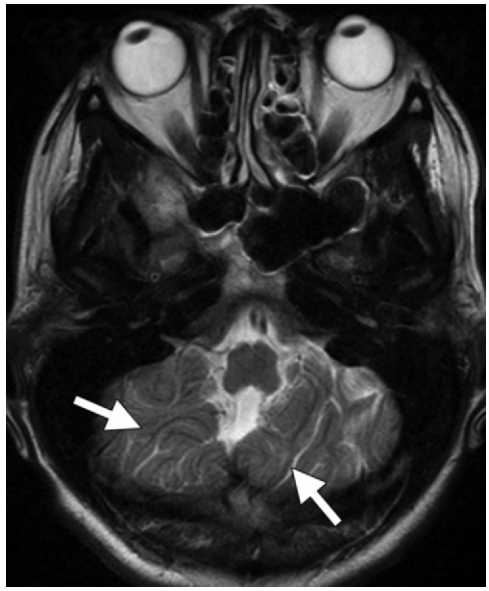

Figure 6. Cerebellar dysplasia in a 17-year-old girl who presented with intellectual disability and seizures. Axial T2-weighted MR image shows abnormal cerebellar foliation and fissuration with loss of the normal white matter architecture in the inferior aspect of the cerebellar hemispheres (arrows).

may be focal or global. Focal findings suggest a disruptive lesion, whereas global findings suggest a malformation. Supratentorial findings, including migrational abnormalities, callosal dysgenesis, and clastic lesions, may also be present (38,39).

Cerebellar dysplasia in the inferior cerebellar hemispheres is a consistent finding in Chudley-McCullough syndrome (OMIM 604213), an autosomal recessive disorder (8). Additional features of Chudley-McCullough syndrome include severe sensorineural hearing loss, mild developmental delay, partial agenesis of the corpus callosum, and periventricular heterotopia (40). Mutations in *GPSM2* have recently been identified as the cause of Chudley-McCullough syndrome (41). This gene encodes a GTPase regulator needed for correct orientation of stem cell division (41).

Cerebellar and Brainstem Malformations

Pontocerebellar Hypoplasia.—As conceptualized by Barth, PCH is a group of autosomal recessive neurodegenerative disorders with a prenatal onset and is characterized by hypoplasia of the cerebellum and pons (11,42). To date, 10 subtypes of PCH with different phenotypes and pathogeneses (types 3 and 8 have a nonprogressive course) have been identified (Table 4) (43–46).

Coronal T2-weighted and sagittal T1- or T2-weighted imaging is essential in the evaluation of PCH (Fig 7). The cerebellar abnormality is characterized by hypoplasia with superimposed atrophy with prenatal onset. In some cases of PCH (particularly type 2, which is caused by mutations in *TSEN54*), there is more severe involvement of the cerebellar hemispheres. On coronal T2-weighted images, this involvement has a "dragonfly" appearance that is created by flattened cerebellar hemispheres (the "wings") and a relatively preserved vermis (the "body") (Fig 7b) (43).

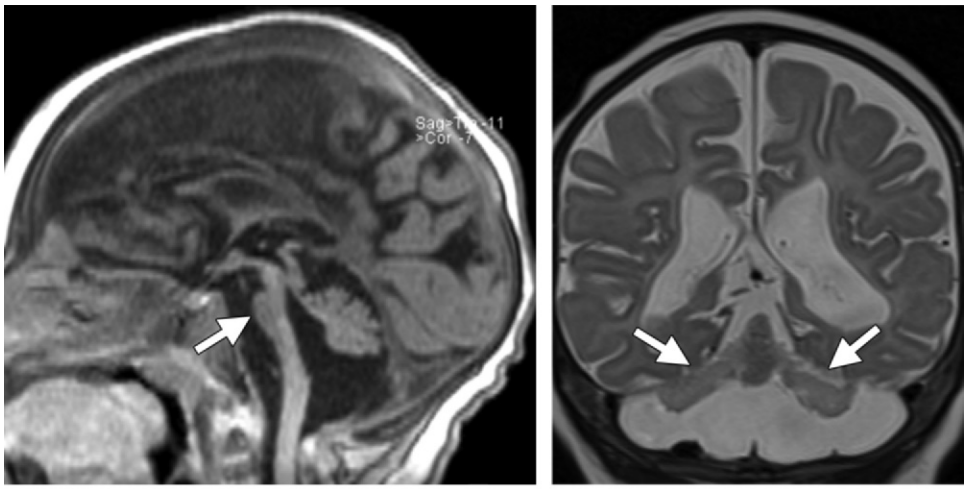

a. b.

Figure 7. PCH type 2 in a 1-year-old child who presented with postnatal progressive microcephaly and dyskinetic movement disorders. **(a)** Sagittal T1-weighted MR image shows hypoplasia of the pons (arrow) and cerebellar vermis. **(b)** Coronal T2-weighted MR image shows reduction in the size of the cerebellar hemispheres (arrows) with relative preservation of the midline vermis, resulting in a characteristic dragonfly appearance.

Absence or significant reduction of the pontine prominence is characteristic of a mid-hindbrain disease with prenatal onset, including malformations, disruptions, or degenerative disorders (47). It is remarkable that hereditary progressive cerebellar disorders causing cerebellar atrophy with postnatal onset do not lead to a significant reduction in pontine size, even in advanced stages. Variable cerebral involvement, including atrophy and delayed myelination, may be present.

The morphologic pattern of pontocerebellar hypoplasia is not specific for PCHs and has also been shown in other selected malformations, disruptions (eg, in extreme prematurity), and neurometabolic diseases (eg, in the congenital disorder known as glycosylation type 1A [OMIM 212065]) (48,49). Patients with mutations in *CASK* present with ataxia, nystagmus, postnatal microcephaly, severe cognitive impairment, and sensorineural hearing loss (50). The neuroimaging correlate includes severe global cerebellar hypoplasia, pontine hypoplasia, reduced gyral pattern, and unmyelinated corpus callosum (51,52). Mutations in *CASK* are inherited with an X-linked pattern. They are lethal in males and occur mostly in females. As mentioned earlier, PCH commonly involves the posterior fossa in migrational disorders and is associated with mutations in *VLDLR* and *RELN* in particular. Finally, PCH is a finding in congenital muscular dystrophies that are caused by defective dystroglycan *O*-glycosylation (discussed later).

Joubert Syndrome.—Joubert syndrome is characterized by hypotonia, ataxia, ocular motor apraxia, neonatal breathing dysregulation, and intellectual disability of variable severity (53,54). The "molar tooth sign" is the diagnostic criterion for Joubert syndrome and consists of elongated, thickened, and horizontally oriented superior cerebellar peduncles; a deep interpeduncular fossa; and vermian hypoplasia (Fig 8a, 8b) (55,56). Systemic involvement may be present and includes renal (nephronophthisis), ocular (colobomas, retinal dystrophy), hepatic (congenital hepatic fibrosis), and skeletal (various forms of polydactyly) involvement. Renal and hepatic involvement may cause high morbidity and mortality in patients with Joubert syndrome and necessitates appropriate work-up and regular follow-up. On the basis of the systemic involvement, six phenotypic subgroups have been described (57). Some degree of phenotype-genotype correlation has been shown between the six phenotypes and the 26 genes associated with Joubert syndrome thus far. All of these genes encode for proteins of the nonmotile primary cilia, which play a key role in the development and functioning of various cells, including retinal photoreceptors, epithelial cells lining the renal tubules and bile ducts, and neurons (54). In the central nervous system, the primary cilia are implicated in neuronal cell proliferation and axonal migration in the cerebellum and brainstem. In almost all patients, Joubert syndrome is inherited with an autosomal recessive pattern and poses a 25% recurrence risk in the affected family (54). Only mutations in *OFD1* are exceptional and inherited with an X-linked pattern.

In Joubert syndrome, the spectrum of neuroimaging findings extends beyond the molar tooth sign and vermian hypoplasia and dys-

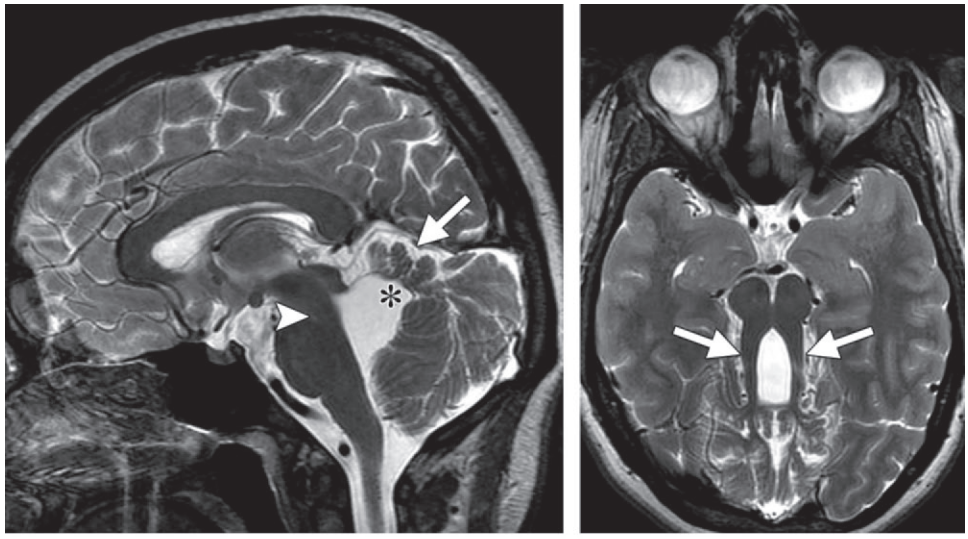

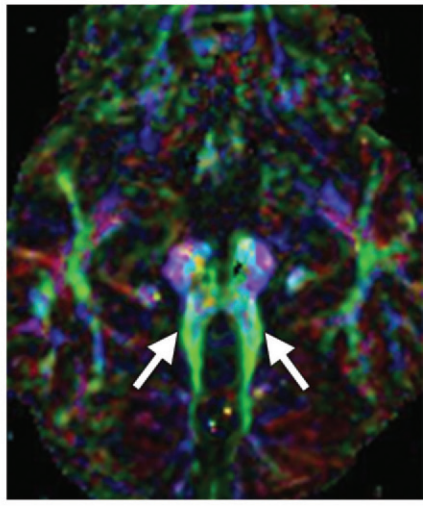

Figure 8. Joubert syndrome in a 5-year-old child who presented with ataxia, ocular motor apraxia, and cognitive impairment. **(a)** Sagittal T2-weighted MR image shows hypoplasia and dysplasia of the vermis (arrow), enlargement of the fourth ventricle with upward and posterior displacement of the fastigium (*), and a narrow pontomesencephalic isthmus (arrowhead). **(b)** Axial T2-weighted MR image shows elongated, thickened, and horizontally oriented superior cerebellar peduncles (arrows) and a deepened interpeduncular fossa, resulting in the characteristic molar tooth sign. **(c)** Axial color-coded fractional anisotropic map obtained at the level of the pontomesencephalic junction shows the horizontal orientation of the superior cerebellar peduncles (green [arrows]) and the absence of decussation of the superior cerebellar peduncles.

plasia, thereby confirming the heterogeneity of Joubert syndrome, not only from the clinical and genetic, but also from the neuroimaging point of view (56). The degree of vermian hypoplasia, form of the molar tooth sign, size of the posterior fossa, and shape and size of the cerebellar hemispheres are variable. Morphologic abnormalities of the brainstem are present in about 30% of patients and include a dysmorphic tectum and midbrain, thickening and elongation of the midbrain, and a small pons (56). Supratentorial involvement occurs in about 30% of patients and includes callosal dysgenesis, cephaloceles, hippocampal malrotation, migrational disorders, and ventriculomegaly (56). Differences in neuroimaging findings may be present in siblings, representing intrafamilial heterogeneity. No correlation between neuroimaging findings and genotype has been found; as a result, neuroimaging findings are of limited value in classifying patients with Joubert syndrome. Only the presence of a hypothalamic hamartoma allows differentiation between oral-facial-digital syndrome type VI and the other five Joubert syndrome subgroups (58).

Diffusion tensor imaging reveals the absence of decussation of the superior cerebellar peduncles and corticospinal tract, which implies an underlying defect in axonal guidance (Fig 8c) (59).

Congenital Muscular Dystrophies Owing to Defective Dystroglycan O-Glycosylation.—The "α-dystroglycanopathies" are a group of congenital muscular dystrophies resulting from mutations in 15 of the genes responsible for the *O*-glycosylation of α-dystroglycan. Mutations in these genes are inherited with an autosomal recessive pattern. The muscles, brain, and eyes are usually affected in α-dystroglycanopathies. Various phenotypes have been described based on the severity of the findings, including Fukuyama disease, muscle-eye-brain disease, and Walker-Warburg syndrome, which is the most severe form (60). However, isolated cerebellar involvement is possible (61).

Weakness, hypotonia, contractures, seizures, cognitive impairment, and eye involvement (eg,

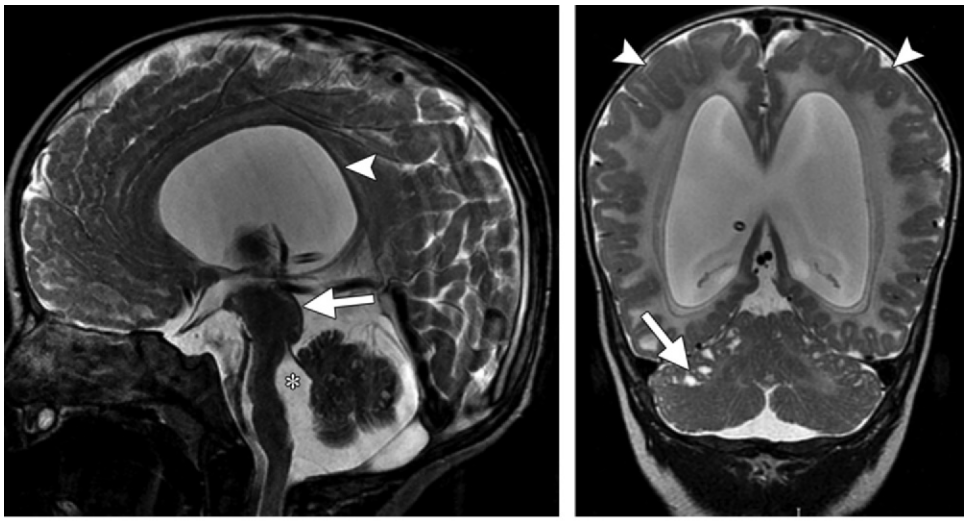

a. b.

Figure 9. Muscle-eye-brain disease and *POMGnT1* mutation in a 5-month-old infant who presented with muscular hypotonia, weakness, intractable seizures, and poor visual function. **(a)** Sagittal T2-weighted MR image shows hypoplasia of the vermis, flattening of the ventral pons, a dysmorphic tectum and midbrain (arrow), an abnormal concave posterior border of the brainstem (*), an enlarged fourth ventricle, and supratentorial ventriculomegaly (arrowhead). **(b)** Coronal T2-weighted MR image shows cerebellar hypoplasia, multiple bilateral subcortical cysts in the cerebellar hemispheres (arrow), cerebellar dysplasia, generalized polymicrogyria (arrowheads), abnormal signal intensity of the supratentorial white matter, absence of the septum pellucidum, and marked ventriculomegaly.

retinal dysplasia and micro-ophthalmia) are common clinical features (62).

Infratentorial involvement includes cerebellar hypoplasia or dysplasia, cerebellar cysts, pontine hypoplasia, ventral pontine cleft, and pontomesencephalic kinking (Fig 9) (60). Cerebellar cysts are a relatively specific finding. These cysts are most likely formed from the portions of the subarachnoid space that were engulfed by the dysplastic cerebellar folia, particularly at the boundary between normal and dysplastic cerebellar cortex (60). Supratentorial involvement ranges from mild ventriculomegaly, diffuse periventricular white matter changes, and focal areas of polymicrogyria (Fig 9b) to severe hydrocephalus, generalized white matter signal changes, and diffuse cortical abnormalities, including cobblestone lissencephaly (60,61).

Predominantly Brainstem Malformations

Pontine Tegmental Cap Dysplasia.—Pontine tegmental cap dysplasia is characterized by a flattened ventral pons, vaulted pontine tegmentum (the "cap"), partial absence of the middle cerebellar peduncles, vermian hypoplasia, a molar tooth–like aspect of the pontomesencephalic junction, and absent inferior olivary prominence (Fig 10a, 10b) (63).

Clinical findings are characterized by the involvement of vestibulocochlear, facial, trigeminal, and glossopharyngeal nerves, resulting in hearing loss, facial paralysis, trigeminal anesthesia, and difficulty in swallowing (63). Systemic involvement with vertebral segmentation anomalies, rib malformations, and congenital heart defects has been observed. The prognosis of pontine tegmental cap dysplasia appears to be highly variable, ranging from mild delay in cognitive development to severe disability (8,64,65). Pontine tegmental cap dysplasia is a sporadic malformation with unknown genotype and no familial recurrence.

Conventional neuroimaging findings are pathognomonic. Diffusion tensor imaging shows absence of the transverse pontine fibers and the presence of a dorsal transverse axonal band at the level of the so-called cap in the dorsal pons (Fig 10c) (63,64,66). The dorsal ectopic axonal band most likely results from abnormal axonal guidance and/or neuronal migration (66).

Horizontal Gaze Palsy with Progressive Scoliosis.—Horizontal gaze palsy with progressive scoliosis (OMIM 607313) is a rare autosomal recessive disorder caused by mutations in *ROBO3*, which encodes a receptor required for axonal guidance (67). Horizontal gaze palsy with progressive scoliosis is characterized clinically by congenital absence of horizontal eye movements, preservation of vertical gaze and convergence, and progressive development of scoliosis in childhood (68).

Neuroimaging reveals a butterfly-shaped medulla due to the missing prominence of the gracile

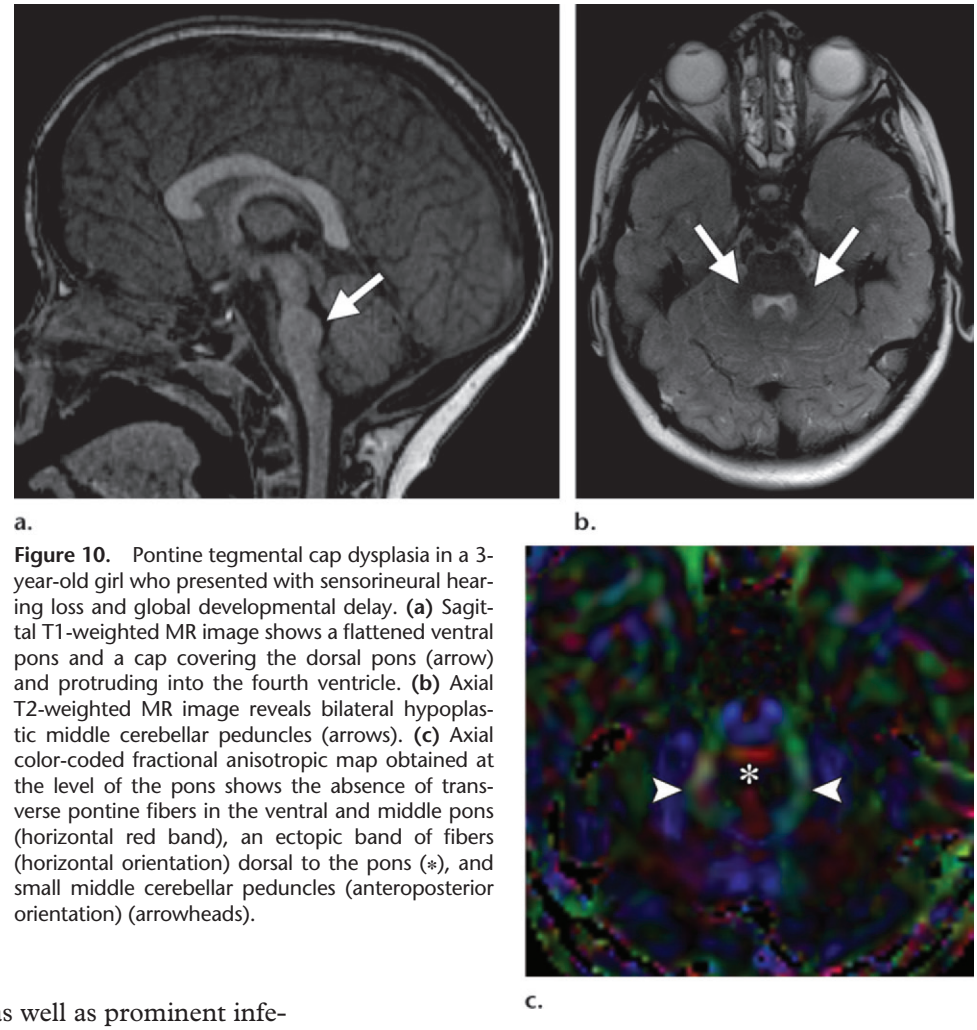

Figure 10. Pontine tegmental cap dysplasia in a 3-year-old girl who presented with sensorineural hearing loss and global developmental delay. **(a)** Sagittal T1-weighted MR image shows a flattened ventral pons and a cap covering the dorsal pons (arrow) and protruding into the fourth ventricle. **(b)** Axial T2-weighted MR image reveals bilateral hypoplastic middle cerebellar peduncles (arrows). **(c)** Axial color-coded fractional anisotropic map obtained at the level of the pons shows the absence of transverse pontine fibers in the ventral and middle pons (horizontal red band), an ectopic band of fibers (horizontal orientation) dorsal to the pons (*), and small middle cerebellar peduncles (anteroposterior orientation) (arrowheads).

and cuneate nuclei, as well as prominent inferior olivary nuclei with respect to the medullary pyramids (69). The pons is hypoplastic and has a dorsal midline cleft with absence of the bulging contour of facial colliculi (69). Diffusion tensor imaging typically shows the absence of decussation of the corticospinal tracts, pontine sensory tracts, and superior cerebellar peduncles (70).

Predominantly Midbrain Malformations

Few disorders that selectively affect the midbrain have been reported. Zaki et al (71) recently reported a new malformation that is characterized by dysplasia of the diencephalic-mesencephalic junction with a butterfly-like contour of the midbrain on axial images.

Cerebellar Disruptions

Cerebellar maturation and adaptation follow a highly orchestrated series of programmed developmental processes of migration, proliferation, and arborization, starting in the middle of the 1st trimester and ending at about 2 years of age (72). The complexity and long duration of cerebellar development place the immature, developing cerebellum at high risk for acquired injury. The cerebellum is particularly vulnerable to metabolic and toxic insults as well as prenatal infections and hemorrhages, whereas it is less vulnerable to prenatal, perinatal, and postnatal hypoxic-ischemic events (5,73).

Cerebellar Agenesis

Cerebellar agenesis is characterized by the near-complete absence of cerebellar tissue. The definition of cerebellar agenesis is based on the morphologic pattern and does not suggest the pathogenesis (5,74). Cerebellar agenesis may represent a malformation resulting from a genetically mediated pathomechanism (eg, mutations in *PTF1A*) or a disruption (eg, hemorrhage that occurs during gestation or in the perinatal period) (5,75).

All patients with cerebellar agenesis are symptomatic. Patients who survive infancy have variable degrees of cerebellar dysfunction (truncal and limb ataxia, dysarthria) as well as cognitive impairment (5). Neonates with cerebellar agenesis should be evaluated for diabetes mellitus, since this association is suggestive of a mutation in *PTF1A* (76).

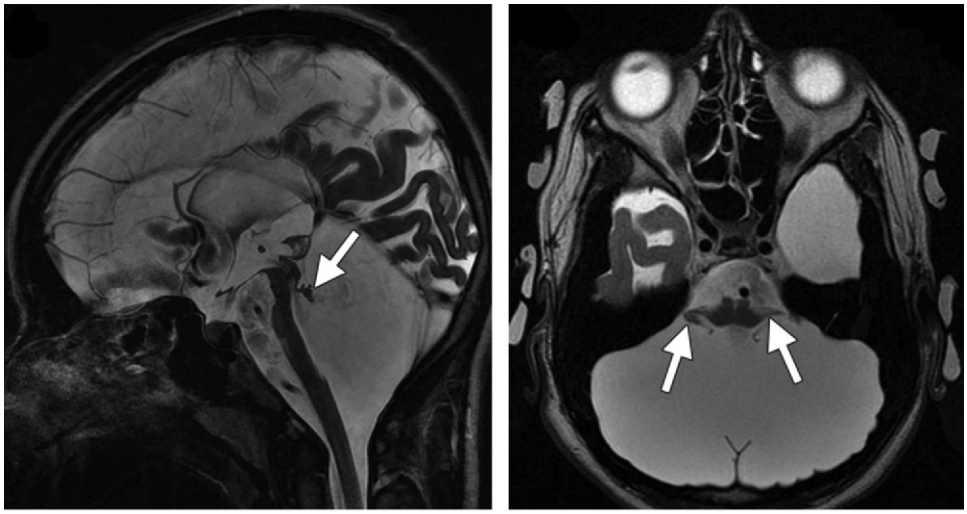

a. b.

Figure 11. Cerebellar agenesis in a 15-year-old girl who presented with severe cognitive impairment and tetraspasticity. **(a)** Sagittal T2-weighted MR image shows near-complete absence of cerebellar structures except for a rudimentary remnant of the anterior vermis (arrow), an enlarged posterior fossa, and marked hypoplasia of the pons. **(b)** Axial T2-weighted MR image shows rudimentary cerebellar tissue (arrows) projecting lateral to the brainstem. (Reprinted, with permission, from reference 5.)

Near-complete absence of cerebellar structures with remnants of the anterior vermis, floccules, and middle cerebellar peduncles are present at neuroimaging (Fig 11). In addition, a secondary pontine hypoplasia and a normal or enlarged posterior fossa may be seen.

Global Cerebellar Hypoplasia

Global cerebellar hypoplasia may result from several causes, both malformations and disruptions; hence, the widely varying clinical presentations and poor correlation with neuroimaging findings. With respect to malformations, global cerebellar hypoplasia has been reported in chromosomal abnormalities (eg, trisomies 13 and 18), metabolic disorders (eg, Zellweger or Smith-Lemli-Opitz syndrome), several genetic syndromes (eg, CHARGE syndrome or velocardiofacial syndrome), and migrational disorders (77). With respect to disruptions, global cerebellar hypoplasia may result from prenatal infections such as CMV or prenatal exposure to anticonvulsant drugs, alcohol, or cocaine (5).

Clinical features and prognosis are heterogeneous and reflect the specific cause. In terms of prognosis and recurrence risk, it is important to identify global cerebellar hypoplasia secondary to a malformation or disruption. This is usually possible on the basis of clinical history and findings as well as additional neuroimaging findings.

Neuroimaging findings show a cerebellum with normal or near-normal shape, but with a reduction in the volume and prominence of the subarachnoid spaces (Fig 12a). Involvement of the vermis and cerebellar hemispheres is typically similar. Ancillary supratentorial findings such as calcification, white matter signal abnormalities, and migrational disorders suggest a prenatal infection such as CMV (Fig 12b).

Unilateral Cerebellar Hypoplasia

Unilateral cerebellar hypoplasia is a rare finding with a spectrum of features ranging from complete aplasia to mild asymmetry in the size of the cerebellar hemispheres (5,78). Increasing experience with prenatal US and fetal MR imaging has demonstrated that unilateral cerebellar hypoplasia is of prenatal origin (and thus represents a disruption), with hemorrhage as the leading cause (5,79).

The most common clinical findings are delayed development and speech, hypotonia, ataxia, and abnormal ocular movements (80). The outcome is variable, ranging from near-normal development to marked motor and intellectual disability. Involvement of the cerebellar vermis is often, but not consistently, associated with a poorer cognitive outcome (78).

Unilateral cerebellar hypoplasia is characterized by variable involvement and volume loss in the cerebellar hemisphere and vermis, with a normal-sized posterior fossa (Fig 13). Evidence of hemorrhage may be present and is best visualized with susceptibility-weighted sequences (10). However, the absence of hemosiderin does not exclude hemorrhage, since the blood-brain barrier is permeable to hemosiderin-laden macrophages between 24–32 weeks gestation. Additional supratentorial disruptive lesions such as porencephalic cysts or clefts may be present and support the disruptive origin of unilateral cerebellar hypoplasia.

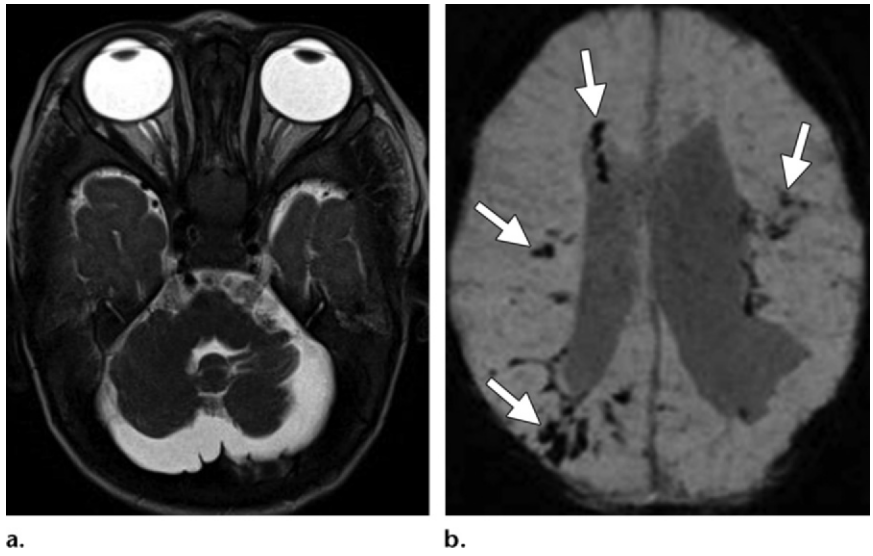

Figure 12. Global cerebellar hypoplasia in a 2-year-old child with a history of congenital CMV infection. The patient presented with impaired motor and cognitive functions, seizures, and sensorineural hearing loss. **(a)** Axial T2-weighted MR image shows global loss of cerebellar volume (more pronounced in the left cerebellar hemisphere) and reduced prominence of the subarachnoid spaces. **(b)** Axial susceptibility-weighted image of the supratentorial brain shows scattered punctate foci of hypointense signal (arrows), suggestive of calcification in the setting of congenital CMV infection.

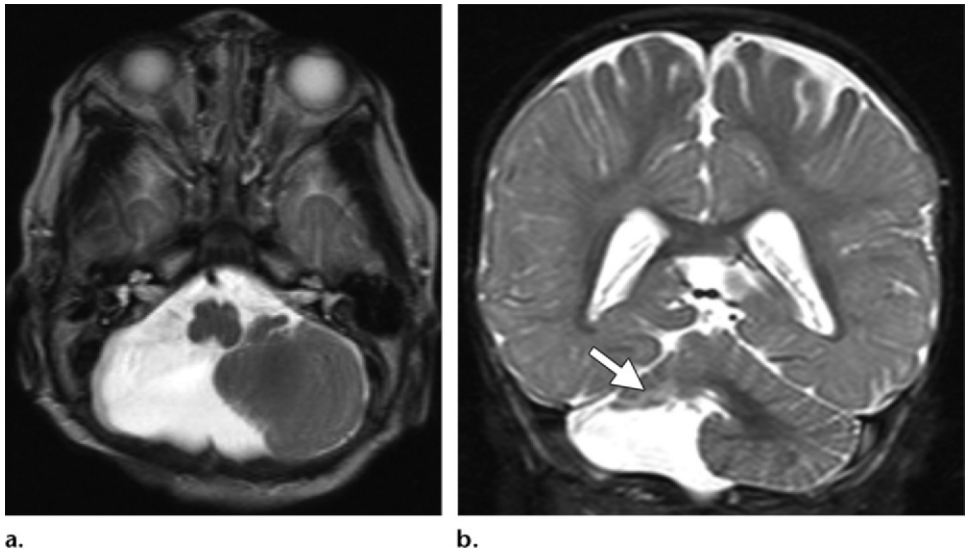

Figure 13. Unilateral cerebellar hypoplasia in a 9-month-old infant who presented with global developmental delay. Axial **(a)** and coronal **(b)** T2-weighted MR images show a normal-appearing left cerebellar hemisphere and near-complete absence of the right cerebellar hemisphere (arrow in **b**).

Cerebellar Cleft

Cerebellar cleft is a rare entity that primarily affects the cerebellar cortical gray matter, extends from the surface of the hemisphere into the parenchyma, and may reach the fourth ventricle, but without involvement of the vermis (81). Cerebellar clefts represent residual disruptive changes, most often secondary to fetal cerebellar hemorrhages (81). Supratentorial disruptive lesions such as schizencephaly may be present and thereby support the disruptive pathomechanism (81).

Clinical findings include language and speech disorders, truncal ataxia, ocular movement disorders, cognitive impairment, and behavioral disorders. The prognosis and outcome depend mostly on the presence and extent of supratentorial lesions.

Typical neuroimaging findings include *(a)* a cleft extending from the surface of the cerebellum through the cerebellar parenchyma toward the fourth ventricle, with malorientation of the cerebellar folia; *(b)* an irregular gray matter–white matter junction; and *(c)* abnormal arborization of the white matter confined to the region adjacent to the cleft, along with volume reduction in the affected hemisphere (Fig 14) (81).

Vanishing Cerebellum in Myelomeningocele

In a non–skin-covered myelomeningocele, prenatal hindbrain herniation through the foramen magnum is believed to be secondary to a prolonged prenatal CSF leak. This herniation may result in parenchymal damage due to ischemia, presumably induced by mechanical distortion, and marked reduction in the size of the cerebellar hemispheres (Fig 15). Boltshauser et al (82) reported this entity in three children with asymmetric involvement of the cerebellar hemispheres and sparing of the vermis.

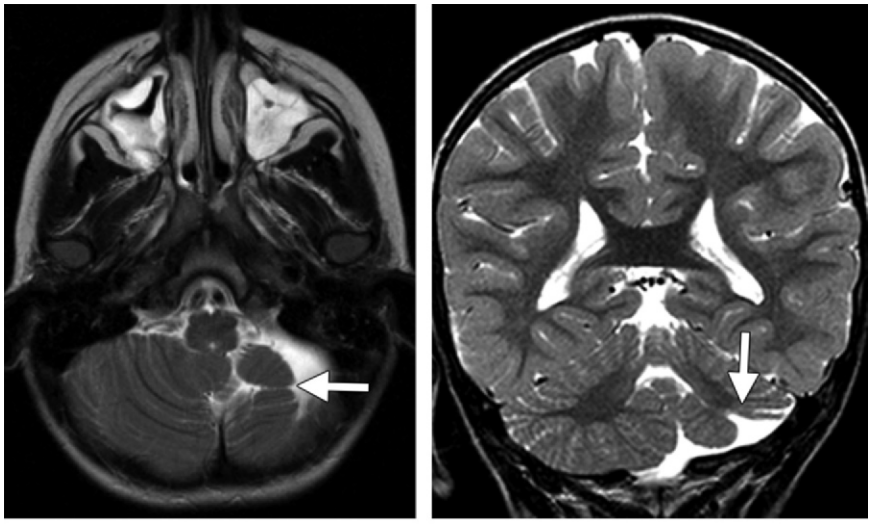

Figure 14. Cerebellar cleft in a 4-year-old girl who presented with mild developmental delay. **(a)** Axial T2-weighted MR image shows reduced volume of the left cerebellar hemisphere with a linear cleft (arrow) running from its surface to the fourth ventricle, along with abnormal cerebellar foliation, fissuration, and white matter arborization around the cleft. **(b)** Coronal T2-weighted MR image shows the cleft in the left cerebellar hemisphere (arrow). The appearance and structure of the vermis and right cerebellar hemisphere are normal.

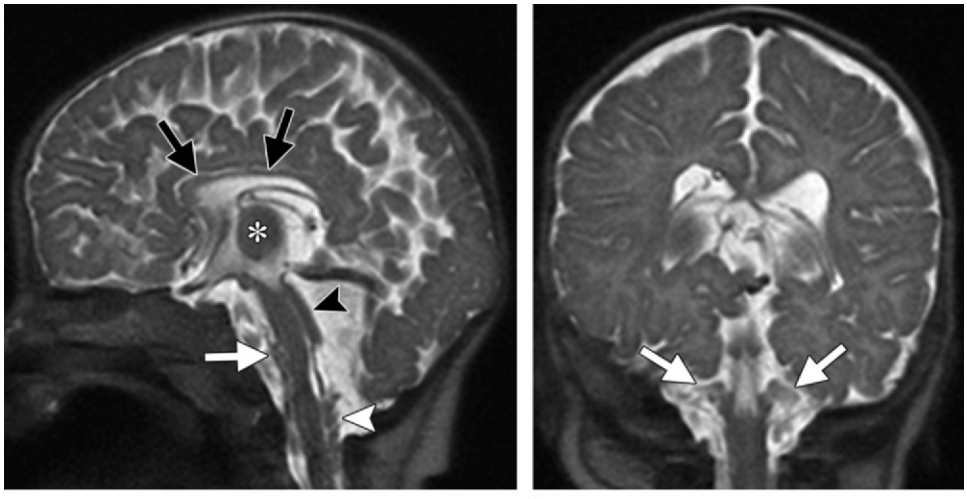

Figure 15. Vanishing cerebellum in a 5-month-old male infant after surgical closure of an open myelomeningocele at birth. **(a)** Sagittal T2-weighted MR image shows a small posterior fossa, flattening of the ventral pons (white arrow), and small remnants of cerebellar tissue herniating into the spinal canal (white arrowhead). Typical findings of a Chiari 2 malformation, including an abnormal tectum (black arrowhead), a prominent massa intermedia (*), and dysgenesis of the corpus callosum (black arrows), are also seen. **(b)** Coronal T2-weighted MR image shows marked reduction in the size of the cerebellar hemispheres, with only small remnants being visualized (arrows).

Cerebellar Disruption or Injury Secondary to Prematurity

During the period from 28 weeks gestation to term, the surface area of the cerebellar cortex increases more than 30-fold (83). This rapid growth of the cerebellum follows a well-programmed developmental process and requires a high degree of energy, placing the developing cerebellum at high risk for injury, particularly during gestational weeks 24–32 (84). Arrested cerebellar development with reduction in the final cerebellar volume is the long-term sequela of cerebellar injuries in preterm neonates (83).

Cerebellar injury occurs in up to 20% of preterm infants prior to 32 weeks gestation (85). Impaired cerebellar development in preterm newborns may be caused by primarily destructive injuries or secondary lesions. Primarily destructive injuries include hemorrhage and ischemia and cause cerebellar tissue loss (86). Secondary lesions lead to underdevelopment of the cerebellum and are caused by direct (eg, hemosiderin–blood products, glucocorticoid exposure, undernutrition) or indirect (impaired transsynaptic trophic effects) effects on the cerebellum (86). General perinatal risk factors for cerebellar injury in extremely premature neonates include prolonged ventilation, pressor support, posthemorrhagic hydrocephalus, and infratentorial hemosiderin deposition (84,87).

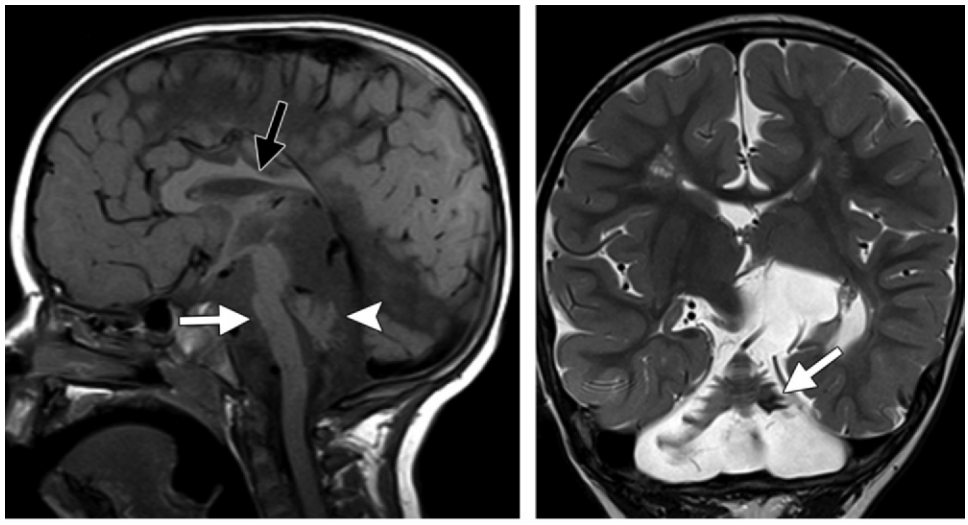

a. b.

Figure 16. Cerebellar disruption in a 3-year-old boy who had been born at 25 weeks gestation and had undergone shunt placement for posthemorrhagic hydrocephalus. **(a)** Sagittal T1-weighted MR image shows a small posterior fossa, a small vermis (arrowhead), and pontine hypoplasia (white arrow). Note also the thin corpus callosum (black arrow), a sequela of prematurity. **(b)** Coronal T2-weighted MR image shows marked reduction in the size of the cerebellar hemispheres, which have a skeletonized appearance; T2 hypointensity of the left folia (arrow), suggestive of remote hemosiderin deposition; and a relatively well-preserved cerebellar vermis compared with the hemispheres. Note also the encephalomalacic changes in the supratentorial brain, a sequela of prematurity.

Surviving preterm neonates with cerebellar injuries have a high prevalence of motor, cognitive, and behavioral disabilities, including autistic features (86).

Typical neuroimaging findings of secondary cerebellar injury include volume reduction that predominantly involves the "skeletonized" cerebellar hemispheres compared with the less affected vermis; a flattened ventral pons; and an enlarged, balloon-shaped fourth ventricle (Fig 16) (49). Hemosiderin deposition may be present and is best depicted with susceptibility-weighted sequences.

Conclusion

Congenital posterior fossa abnormalities represent a wide variety of disorders that include both malformations and disruptions. These disorders may involve a single structure within the posterior fossa (eg, the cerebellum alone) or a combination of structures (eg, the pons and cerebellum). Neuroimaging yields detailed anatomic findings and plays a key role in the diagnosis of congenital posterior fossa abnormalities. Well-defined neuroimaging-based diagnostic criteria are available for the various disorders and should be used by pediatric neurologists, general radiologists, and neuroradiologists. Accurate classification of congenital posterior fossa abnormalities is important for therapy, prognosis, and genetic counseling. If the diagnostic criteria for well-defined anomalies are not met, a detailed anatomic description is to be preferred, and confusing terms that lack specificity (eg, Dandy-Walker variant, Dandy-Walker spectrum) should be avoided or, even better, abandoned.

References

1. Patel S, Barkovich AJ. Analysis and classification of cerebellar malformations. AJNR Am J Neuroradiol 2002;23(7):1074–1087.
2. Parisi MA, Dobyns WB. Human malformations of the midbrain and hindbrain: review and proposed classification scheme. Mol Genet Metab 2003;80(1-2):36–53.
3. Barkovich AJ, Millen KJ, Dobyns WB. A developmental and genetic classification for midbrain-hindbrain malformations. Brain 2009;132(pt 12):3199–3230.
4. Boltshauser E. Cerebellum: small brain but large confusion—a review of selected cerebellar malformations and disruptions. Am J Med Genet A 2004;126A(4):376–385.
5. Poretti A, Prayer D, Boltshauser E. Morphological spectrum of prenatal cerebellar disruptions. Eur J Paediatr Neurol 2009;13(5):397–407.
6. Hennekam RC, Biesecker LG, Allanson JE, et al. Elements of morphology: general terms for congenital anomalies. Am J Med Genet A 2013;161A(11):2726–2733.
7. de Vries LS, Mancini GM. Intracerebral hemorrhage and COL4A1 and COL4A2 mutations, from fetal life into adulthood. Ann Neurol 2012;71(4):439–441.
8. Doherty D, Millen KJ, Barkovich AJ. Midbrain and hindbrain malformations: advances in clinical diagnosis, imaging, and genetics. Lancet Neurol 2013;12(4):381–393.
9. Poretti A, Meoded A, Rossi A, Raybaud C, Huisman TA. Diffusion tensor imaging and fiber tractography in brain malformations. Pediatr Radiol 2013;43(1):28–54.
10. Bosemani T, Poretti A, Huisman TA. Susceptibility-weighted imaging in pediatric neuroimaging. J Magn Reson Imaging 2014;40(3):530–544.
11. Barth PG. Pontocerebellar hypoplasias: an overview of a group of inherited neurodegenerative disorders with fetal onset. Brain Dev 1993;15(6):411–422.
12. Kumar R, Jain MK, Chhabra DK. Dandy-Walker syndrome: different modalities of treatment and outcome in 42 cases. Childs Nerv Syst 2001;17(6):348–352.

13. Alexiou GA, Sfakianos G, Prodromou N. Dandy-Walker malformation: analysis of 19 cases. J Child Neurol 2010;25(2):188–191.
14. Boddaert N, Klein O, Ferguson N, et al. Intellectual prognosis of the Dandy-Walker malformation in children: the importance of vermian lobulation. Neuroradiology 2003; 45(5):320–324.
15. Bolduc ME, Limperopoulos C. Neurodevelopmental outcomes in children with cerebellar malformations: a systematic review. Dev Med Child Neurol 2009;51(4):256–267.
16. Tortori-Donati P, Fondelli MP, Rossi A, Carini S. Cystic malformations of the posterior cranial fossa originating from a defect of the posterior membranous area: mega cisterna magna and persisting Blake's pouch—two separate entities. Childs Nerv Syst 1996;12(6):303–308.
17. Nelson MD Jr, Maher K, Gilles FH. A different approach to cysts of the posterior fossa. Pediatr Radiol 2004;34(9): 720–732.
18. Cornips EM, Overvliet GM, Weber JW, et al. The clinical spectrum of Blake's pouch cyst: report of six illustrative cases. Childs Nerv Syst 2010;26(8):1057–1064.
19. Poretti A, Scheer I, Boltshauser E. Posterior fossa cysts and cyst-like malformations (Blake's pouch cyst, arachnoid cysts, and mega cisterna magna). In: Boltshauser E, Schmahmann JD, eds. Cerebellar disorders in children. London, England: Mac Keith, 2012; 212–216.
20. Yildiz H, Yazici Z, Hakyemez B, Erdogan C, Parlak M. Evaluation of CSF flow patterns of posterior fossa cystic malformations using CSF flow MR imaging. Neuroradiology 2006;48(9):595–605.
21. Barkovich AJ, Kjos BO, Norman D, Edwards MS. Revised classification of posterior fossa cysts and cystlike malformations based on the results of multiplanar MR imaging. AJR Am J Roentgenol 1989;153(6):1289–1300.
22. Ali ZS, Lang SS, Bakar D, Storm PB, Stein SC. Pediatric intracranial arachnoid cysts: comparative effectiveness of surgical treatment options. Childs Nerv Syst 2014;30(3):461–469.
23. Marin-Sanabria EA, Yamamoto H, Nagashima T, Kohmura E. Evaluation of the management of arachnoid cyst of the posterior fossa in pediatric population: experience over 27 years. Childs Nerv Syst 2007;23(5):535–542.
24. Estroff JA, Scott MR, Benacerraf BR. Dandy-Walker variant: prenatal sonographic features and clinical outcome. Radiology 1992;185(3):755–758.
25. Limperopoulos C, Robertson RL, Estroff JA, et al. Diagnosis of inferior vermian hypoplasia by fetal magnetic resonance imaging: potential pitfalls and neurodevelopmental outcome. Am J Obstet Gynecol 2006;194(4):1070–1076.
26. Tarui T, Limperopoulos C, Sullivan NR, Robertson RL, du Plessis AJ. Long-term developmental outcome of children with a fetal diagnosis of isolated inferior vermian hypoplasia. Arch Dis Child Fetal Neonatal Ed 2014;99(1):F54–F58.
27. Jissendi-Tchofo P, Kara S, Barkovich AJ. Midbrain-hindbrain involvement in lissencephalies. Neurology 2009;72(5): 410–418.
28. Hong SE, Shugart YY, Huang DT, et al. Autosomal recessive lissencephaly with cerebellar hypoplasia is associated with human RELN mutations. Nat Genet 2000;26(1):93–96. [Published correction appears in Nat Genet 2001;27(2):225.]
29. Boycott KM, Flavelle S, Bureau A, et al. Homozygous deletion of the very low density lipoprotein receptor gene causes autosomal recessive cerebellar hypoplasia with cerebral gyral simplification. Am J Hum Genet 2005;77(3):477–483.
30. Cushion TD, Dobyns WB, Mullins JG, et al. Overlapping cortical malformations and mutations in TUBB2B and TUBA1A. Brain 2013;136(pt 2):536–548.
31. Toelle SP, Yalcinkaya C, Kocer N, et al. Rhombencephalosynapsis: clinical findings and neuroimaging in 9 children. Neuropediatrics 2002;33(4):209–214.
32. Poretti A, Alber FD, Bürki S, Toelle SP, Boltshauser E. Cognitive outcome in children with rhombencephalosynapsis. Eur J Paediatr Neurol 2009;13(1):28–33.
33. Sukhudyan B, Jaladyan V, Melikyan G, Schlump JU, Boltshauser E, Poretti A. Gómez-López-Hernández syndrome: reappraisal of the diagnostic criteria. Eur J Pediatr 2010;169(12):1523–1528.
34. Ishak GE, Dempsey JC, Shaw DW, et al. Rhombencephalosynapsis: a hindbrain malformation associated with incomplete separation of midbrain and forebrain, hydrocephalus and a broad spectrum of severity. Brain 2012;135(pt 5):1370–1386.
35. Poretti A, Mall V, Smitka M, et al. Macrocerebellum: significance and pathogenic considerations. Cerebellum 2012;11(4):1026–1036.
36. Alqahtani E, Huisman TA, Boltshauser E, et al. Mucopolysaccharidoses type I and II: new neuroimaging findings in the cerebellum. Eur J Paediatr Neurol 2014;18(2):211–217.
37. Poretti A, Boltshauser E. Macrocerebellum. In: Boltshauser E, Schmahmann JD, eds. Cerebellar disorders in children. London, England: Mac Keith, 2012; 192–194.
38. Poretti A, Boltshauser E. Cerebellar dysplasia. In: Boltshauser E, Schmahmann JD, eds. Cerebellar disorders in children. London, England: Mac Keith, 2012; 172–176.
39. Demaerel P. Abnormalities of cerebellar foliation and fissuration: classification, neurogenetics and clinicoradiological correlations. Neuroradiology 2002;44(8):639–646.
40. Chudley AE, McCullough C, McCullough DW. Bilateral sensorineural deafness and hydrocephalus due to foramen of Monro obstruction in sibs: a newly described autosomal recessive disorder. Am J Med Genet 1997;68(3):350–356.
41. Doherty D, Chudley AE, Coghlan G, et al. GPSM2 mutations cause the brain malformations and hearing loss in Chudley-McCullough syndrome. Am J Hum Genet 2012;90(6):1088–1093. [Published correction appears in Am J Hum Genet 2012;91(1):209.]
42. Namavar Y, Barth PG, Kasher PR, et al. Clinical, neuroradiological and genetic findings in pontocerebellar hypoplasia. Brain 2011;134(pt 1):143–156.
43. Namavar Y, Barth PG, Poll-The BT, Baas F. Classification, diagnosis and potential mechanisms in pontocerebellar hypoplasia. Orphanet J Rare Dis 2011;6:50.
44. Mochida GH, Ganesh VS, de Michelena MI, et al. CHMP1A encodes an essential regulator of BMI1-INK4A in cerebellar development. Nat Genet 2012;44(11):1260–1264.
45. Akizu N, Cantagrel V, Schroth J, et al. AMPD2 regulates GTP synthesis and is mutated in a potentially treatable neurodegenerative brainstem disorder. Cell 2013;154 (3):505–517.
46. Schaffer AE, Eggens VR, Caglayan AO, et al. CLP1 founder mutation links tRNA splicing and maturation to cerebellar development and neurodegeneration. Cell 2014;157(3):651–663.
47. Poretti A, Wolf NI, Boltshauser E. Differential diagnosis of cerebellar atrophy in childhood. Eur J Paediatr Neurol 2008;12(3):155–167.
48. Feraco P, Mirabelli-Badenier M, Severino M, et al. The shrunken, bright cerebellum: a characteristic MRI finding in congenital disorders of glycosylation type 1a. AJNR Am J Neuroradiol 2012;33(11):2062–2067.
49. Messerschmidt A, Brugger PC, Boltshauser E, et al. Disruption of cerebellar development: potential complication of extreme prematurity. AJNR Am J Neuroradiol 2005;26(7):1659–1667.
50. Najm J, Horn D, Wimplinger I, et al. Mutations of CASK cause an X-linked brain malformation phenotype with microcephaly and hypoplasia of the brainstem and cerebellum. Nat Genet 2008;40(9):1065–1067.
51. Takanashi J, Arai H, Nabatame S, et al. Neuroradiologic features of CASK mutations. AJNR Am J Neuroradiol 2010;31(9):1619–1622.
52. Burglen L, Chantot-Bastaraud S, Garel C, et al. Spectrum of pontocerebellar hypoplasia in 13 girls and boys with CASK mutations: confirmation of a recognizable phenotype and first description of a male mosaic patient. Orphanet J Rare Dis 2012;7:18.
53. Doherty D. Joubert syndrome: insights into brain development, cilium biology, and complex disease. Semin Pediatr Neurol 2009;16(3):143–154.
54. Romani M, Micalizzi A, Valente EM. Joubert syndrome: congenital cerebellar ataxia with the molar tooth. Lancet Neurol 2013;12(9):894–905.
55. Gleeson JG, Keeler LC, Parisi MA, et al. Molar tooth sign of the midbrain-hindbrain junction: occurrence in multiple distinct syndromes. Am J Med Genet A 2004;125A(2):125–134; discussion 117.

56. Poretti A, Huisman TA, Scheer I, Boltshauser E. Joubert syndrome and related disorders: spectrum of neuroimaging findings in 75 patients. AJNR Am J Neuroradiol 2011;32(8):1459–1463.
57. Brancati F, Dallapiccola B, Valente EM. Joubert syndrome and related disorders. Orphanet J Rare Dis 2010;5:20.
58. Poretti A, Vitiello G, Hennekam RC, et al. Delineation and diagnostic criteria of oral-facial-digital syndrome type VI. Orphanet J Rare Dis 2012;7:4.
59. Poretti A, Boltshauser E, Loenneker T, et al. Diffusion tensor imaging in Joubert syndrome. AJNR Am J Neuroradiol 2007;28(10):1929–1933.
60. Clement E, Mercuri E, Godfrey C, et al. Brain involvement in muscular dystrophies with defective dystroglycan glycosylation. Ann Neurol 2008;64(5):573–582.
61. Poretti A, Häusler M, von Moers A, et al. Ataxia, intellectual disability, and ocular apraxia with cerebellar cysts: a new disease? Cerebellum 2014;13(1):79–88.
62. Godfrey C, Clement E, Mein R, et al. Refining genotype phenotype correlations in muscular dystrophies with defective glycosylation of dystroglycan. Brain 2007;130(pt 10): 2725–2735.
63. Barth PG, Majoie CB, Caan MW, et al. Pontine tegmental cap dysplasia: a novel brain malformation with a defect in axonal guidance. Brain 2007;130(pt 9):2258–2266.
64. Briguglio M, Pinelli L, Giordano L, et al. Pontine tegmental cap dysplasia: developmental and cognitive outcome in three adolescent patients. Orphanet J Rare Dis 2011;6:36.
65. Rauscher C, Poretti A, Neuhann TM, et al. Pontine tegmental cap dysplasia: the severe end of the clinical spectrum. Neuropediatrics 2009;40(1):43–46.
66. Jissendi-Tchofo P, Doherty D, McGillivray G, et al. Pontine tegmental cap dysplasia: MR imaging and diffusion tensor imaging features of impaired axonal navigation. AJNR Am J Neuroradiol 2009;30(1):113–119.
67. Jen JC, Chan WM, Bosley TM, et al. Mutations in a human ROBO gene disrupt hindbrain axon pathway crossing and morphogenesis. Science 2004;304(5676):1509–1513.
68. Rossi A, Catala M, Biancheri R, Di Comite R, Tortori-Donati P. MR imaging of brain-stem hypoplasia in horizontal gaze palsy with progressive scoliosis. AJNR Am J Neuroradiol 2004;25(6):1046–1048.
69. Bosley TM, Salih MA, Jen JC, et al. Neurologic features of horizontal gaze palsy and progressive scoliosis with mutations in ROBO3. Neurology 2005;64(7):1196–1203.
70. Sicotte NL, Salamon G, Shattuck DW, et al. Diffusion tensor MRI shows abnormal brainstem crossing fibers associated with ROBO3 mutations. Neurology 2006;67(3):519–521.
71. Zaki MS, Saleem SN, Dobyns WB, et al. Diencephalic-mesencephalic junction dysplasia: a novel recessive brain malformation. Brain 2012;135(pt 8):2416–2427.
72. Limperopoulos C. Cerebellar injury in the preterm infant. In: Boltshauser E, Schmahmann JD, eds. Cerebellar disorders in children. London, England: Mac Keith, 2011; 314–321.
73. Boltshauser E. Cerebellar imaging: an important signpost in paediatric neurology. Childs Nerv Syst 2001;17(4-5): 211–216.
74. Reardon W, Donnai D. Dysmorphology demystified. Arch Dis Child Fetal Neonatal Ed 2007;92(3):F225–F229.
75. Sellick GS, Barker KT, Stolte-Dijkstra I, et al. Mutations in PTF1A cause pancreatic and cerebellar agenesis. Nat Genet 2004;36(12):1301–1305.
76. Hoveyda N, Shield JP, Garrett C, et al. Neonatal diabetes mellitus and cerebellar hypoplasia/agenesis: report of a new recessive syndrome. J Med Genet 1999;36(9):700–704.
77. Poretti A, Boltshauser E, Doherty D. Cerebellar hypoplasia: differential diagnosis and diagnostic approach. Am J Med Genet C Semin Med Genet 2014;166(2):211–226 .
78. Poretti A, Limperopoulos C, Roulet-Perez E, et al. Outcome of severe unilateral cerebellar hypoplasia. Dev Med Child Neurol 2010;52(8):718–724.
79. Massoud M, Cagneaux M, Garel C, et al. Prenatal unilateral cerebellar hypoplasia in a series of 26 cases: significance and implications for prenatal diagnosis. Ultrasound Obstet Gynecol 2014;44(4):447–454.
80. Benbir G, Kara S, Yalcinkaya BC, et al. Unilateral cerebellar hypoplasia with different clinical features. Cerebellum 2011;10(1):49–60.
81. Poretti A, Huisman TA, Cowan FM, et al. Cerebellar cleft: confirmation of the neuroimaging pattern. Neuropediatrics 2009;40(5):228–233.
82. Boltshauser E, Schneider J, Kollias S, Waibel P, Weissert M. Vanishing cerebellum in myelomeningocele. Eur J Paediatr Neurol 2002;6(2):109–113.
83. Limperopoulos C, Soul JS, Gauvreau K, et al. Late gestation cerebellar growth is rapid and impeded by premature birth. Pediatrics 2005;115(3):688–695.
84. Messerschmidt A, Prayer D, Brugger PC, et al. Preterm birth and disruptive cerebellar development: assessment of perinatal risk factors. Eur J Paediatr Neurol 2008;12(6):455–460.
85. Steggerda SJ, Leijser LM, Wiggers-de Bruïne FT, van der Grond J, Walther FJ, van Wezel-Meijler G. Cerebellar injury in preterm infants: incidence and findings on US and MR images. Radiology 2009;252(1):190–199.
86. Volpe JJ. Cerebellum of the premature infant: rapidly developing, vulnerable, clinically important. J Child Neurol 2009;24(9):1085–1104.
87. Limperopoulos C, Benson CB, Bassan H, et al. Cerebellar hemorrhage in the preterm infant: ultrasonographic findings and risk factors. Pediatrics 2005;116(3):717–724.